# An Investigation into the Colored Stochastic Hodgkin-Huxley Equations Under Noisy Input Currents

**Ahmed Mahmood Khudhur**

Submitted to the
Institute of Graduate Studies and Research
in partial fulfillment of the requirements for the Degree of

Master of Science
in
Computer Engineering

Eastern Mediterranean University
March 2014
Gazimağusa, North Cyprus

Approval of the Institute of Graduate Studies and Research

Prof. Dr. Elvan Yılmaz
Director

I certify that this thesis satisfies the requirements as a thesis for the degree of Master of Science in Computer Engineering.

Prof. Dr. Işık Aybay
Chair, Department of Computer Engineering

We certify that we have read this thesis and that in our opinion it is fully adequate in scope and quality as a thesis for the degree of Master of Science in Computer Engineering.

Prof. Dr. Marifi Güler
Supervisor

Examining Committee

1. Prof. Dr. Marifi Güler
2. Asst. Prof. Dr. Cem Ergün
3. Asst. Prof. Dr. Ahmet Ünveren

# ABSTRACT

In recent years, it has been argued and shown experimentally that ion channel noise in neurons can have profound influence on the neuron's dynamical behavior. Most profoundly, ion channel noise was seen to be able to cause spontaneous firing and stochastic resonance.

It was recently found by Güler (2011) that a non-trivially persistent correlation takes place between the transmembrane voltage fluctuations and the element of open channel fluctuations attributed to the gate multiplicity. This non-trivial phenomenon was found to be playacting an essential important role for the elevation of excitability and spontaneous firing in the small size cell. In addition, the same phenomenon was found to be enhancing the spike coherence significantly. More recently, the effects of the above cross correlation persistency was modeled; by the same author M. Güler (2013), through inserting some colored noise terms inside the conductances in the stochastic Hodgkin- Huxley equations.

In this thesis, the colored stochastic Hodgkin-Huxley equations were studied when the input current to the neuron is noisy. The spiking rates and the spike coherence were examined. In particular, the role played by the presence of the colored noise terms in the conductances was focused on in the examination. Our investigation reveals that the presence of the colored noise terms enhances the agreement with the microscopic simulation results not only in the case of the noise-free input currents but also in the case of the noisy currents.

**Keywords:** ion channel, channel noise, colored noise, channel gate, small size membrane, stochastic Hodgkin-Huxley

# ÖZ

Son yıllarda, nöronlardaki ion kanal gürültüsünün nöron dinamiği üzerinde hayati etki yapabildiği deneysel olarak da kanıtlanmıştır. Bu kapsamda, kendi kendine ateşleme ve stokastik rezonans en çarpıcı bulgulardır.

İyon kanallarında çoklu geçit bulunmasının, voltage dalgalanmaları ve açık kanal dalgalanmaları arasında ilk bakışta gözükmeyen bir daimi çapraz ilişkiye neden olduğu Güler (2011) tarafından ortaya çıkartılmıştır. Bu ilk bakışta gözükmeyen olgunun, küçük boyutlu hücrelerde yüksek uyarılma ve kendi kendine ateşlemeye neden olduğu bulunmuştur. İlaveten, sözkonusu olgunun ateşleme uyumluluğunu arttırdığı saptanmıştır. Daha yakın zamanda, Fox ve Lu'nun stokastik Hodgkin-Huxley denklemleri geçirgenliklere renkli gürültü terimleri ekleyerek genişletilmiştir (Güler, 2013).

Bu tezde, yukarıdaki renklendirilmiş stokastik Hodgkin-Huxley modeli, gürültülü girdi akımları kullanılarak çalışılmıştır. Renkli gürültü terimlerinin varlığının gürültülü girdi akımları kullanılması durumunda da mikroskopik benzeşim sonuçlarıyla uyumu arttırdığı gözlenmiştir.

**Anahtar Kelimeler:** İyon kanalı, Kanal gürültüsü, Renkli gürültü, Kanal geçiti, Küçük boyutlu zar, Stokastik Hodgkin-Huxley.

**I lovingly dedicate this thesis**

**To my beloved father**

**To my beloved mother**

**To my brother and sisters**

**To all my friend**

# ACKNOWLEDGMENT

I would like to thank all those who helped me throughout my research. I am particularly thankful to my supervisor, Prof. Dr. Marifi GÜLER , for giving me the opportunity to undertake this research assignment, and, most importantly, for his invaluable advice, continuous encouragement, and patient guidance.

Special thanks to my beloved father, e.g. Mahmood Khudhur Salman, and to my beloved mother precious, and to my sisters, Hind, Zainab and Maha and my brother Ali and to all my friends for their support and helping me.

# TABLE OF CONTENTS

# LIST OF TABLES

# LIST OF FIGURES

# Chapter 1

# INTRODUCTION

Effectiveness of noise to the neurons produces an unusual pattern on the neuronal dynamics. The noise is in two types; internal or external (Faisal A. S., 2008). External noise is exactly the opposite of internal. External noise is produced from the synaptic transmission also from network effects. The major source of internal noise is due to the existence of a finite number of voltage-gated ion channels in a patch of neuronal membrane. These channels are water filled holes in the cell membrane that are formed by proteins embedded in the lipid bilayer, with the property that each type of ion channel is selective to conduct a particular ion species (Hille, 2001).

They play a fundamental physiological role for the excitability of cells where the conductance of potassium and sodium is facilitated by voltage-gated ion channels. The number of open channels fluctuates in a seemingly random manner (Sakmann, 1995) implying a fluctuation in the conductivity of the membrane, which, in turn, implies a fluctuation in the transmembrane voltage.

In the case of having a large number of ion channels means that the membrane size is huge, then the voltage dynamics will represent as it is in the original Hodgkin and Huxley (Hodgkin, 1952) equation. However, when the patch of membrane is small, the conductance fluctuations affect the voltage activity of the cell. These effects are probably important and cannot be ignored. The single open channel stochasticity

effect in a direct manner the spike behavior which is suggested by experimental investigation((Sigworth, 1980); (Lynch, 1989); (Johansson, 1994)), and spontaneous fire will be the result of that noise in the ion channels ((Koch, 1999);(White, 1998)). Patch-clamp investigates in Lab explained, the noise of channel in the dendrites also in the soma resulting voltage change in variation strong adequate cause asynchronies in the timing, initiation, and propagation of action potentials ((Diba, 2004); (Jacobson, 2005); (Dorval, 2005); (Kole, 2006)). In the voltage-dependent ion channel system, as a consequence this phenomenon is produced and called stochastic resonance created from the peptide alamethicin(Bezrukov, 1995).

Spontaneous spiking is a phenomenon caused by the internal noise from the ion channels. Proof through theoretical investigations and numerical simulations of channel dynamics( in repeating manner ), or in some other cause quiet membrane patches((DeFelice, 1992); (Strassberg, 1993); (Chow, 1996); (Rowat, 2004); (Güler, 2007) ;(Güler, 2008);(Güler, 2011); (Güler, 2013)); and also these investigations and the simulations have shown the status of stochastic reflection and the cohesion of produced spike trains ((Jung, 2001); (Schmid, 2001); (Özer, 2006)).

In addition, the channel fluctuations might reach the critical value near from the action potential threshold even if the numbers of existed ion channels are large. ((Schneidman, 1998); (Rubinstein, 1995)); The timing accuracy of an action potential is measured by a small number of opening ion channel at that threshold. Furthermore, ion channel noise controls the spike propagation in axons ((Faisal A. A., 2007); (Ochab-Marcinek, 2009)).

It has been revealed in earlier theoretical experiments (Güler. 2011) that it is not just the gate noise (the quantity of fluctuations in the open gates') that affects neuron's behavior, but also the existence of a large quantity of gates in single ion channel, Furthermore this effect that may be pointing on an important role in activity within the cell in case of having membrane bounded in size.

More recently, a stochastic Hodgkin – Huxley model, having colored noise terms in the conductances was proposed (Güler, 2013), where the colored terms capture those effects due to the gate multiplicity.

## 1.1 Scope and Organization

In this thesis, the colored stochastic Hodgkin Huxley equations, introduced by Güler (2013) will be studied when the input current to the neuron is noisy. In particular, the role played by the present of the colored noise term in the conductances will be focused on in the examination. Chapter one contains the introduction, chapter two handles Biological principles and neuron structure, in chapter three the Hodgkin Huxley equation is dealt with, chapter 4 contains the membrane dynamics, chapter 5 includes the Güler model formulations and noise variance, spike coherence, and chapter 6 includes the experiments and results of the study.

# Chapter 2

# BIOLOGICAL PRINCIPLES

The brain structure and its organisation have been attracting attention through all history. Because of the brain's incredible connectivity and the microscopic scale of its interconnection, there is lack consistent theories about neural coding and computation in modern neuroscience. The investigation of neuron structure is an incredibly difficult and complex task that yields relatively low rewards in terms of information from biological forms. The structure and connectivity of even the simplest invertebrates are almost impossible to establish with standard laboratory techniques. That is why at present knowledge about the operational principles of the brain is far from complete, so simulation attempts must employ a great deal of assumption and guesswork to fill the gaps in the experimental evidence. Understanding of the principles and mechanisms of brain activity could benefit the human development. First of all, imitation could allow expanding of computing capabilities. Also, understanding such a phenomenon as memory capacity, an animal's planning or reasoning, thought or consciousness (particularly mammals) would benefit the progress of the mankind. Finally, the hope is that by emulating the brain, it will be possible to capture some of its computing capabilities. The main feature of the brain is the ability to learn. We understand learning as the probability for certain behaviour to happen in response to a certain event.

The basis for most models of learning is a synaptic plasticity. Plasticity refers to the changes that occur in the organisation of the brain as a result of experience. Several underlying mechanisms cooperate to achieve plasticity, forming cognition and memory formation.

## 2.1 Neuron Structure

In order to imitate biological neural networks it is important to understand the nature of biological neurons, which are the building blocks of neural networks. This section introduces biological neurons and explains how they work. The investigation of the neuron behaviour is an incredibly difficult and complex task. It is almost impossible to establish the brain's structure and connectivity of even an elementary animal using conventional laboratory techniques. Recent research employed alternative ways of investigations using electro-physiological techniques and computer simulation experiments (A. G. Guggisberg, 2008). They unveiled the internal structure of the brain and allowed the scientists to mimic its behaviour. Although there are all kinds of different neurons, the basic structure is the same. As an ordinary cell, a neuron typically consists of a soma (or cell body), a dendric tree and an axon. The majority of the neurons in vertebrate organisms input the signal through the synapses on the dendrites, transmit it along the cell body outputting via the synapses located on the axon. However, there is some heterogeneity throughout the nervous system of different species in the size, shape and function of neurons. The key parts of the neuron are shown in Figure 1.

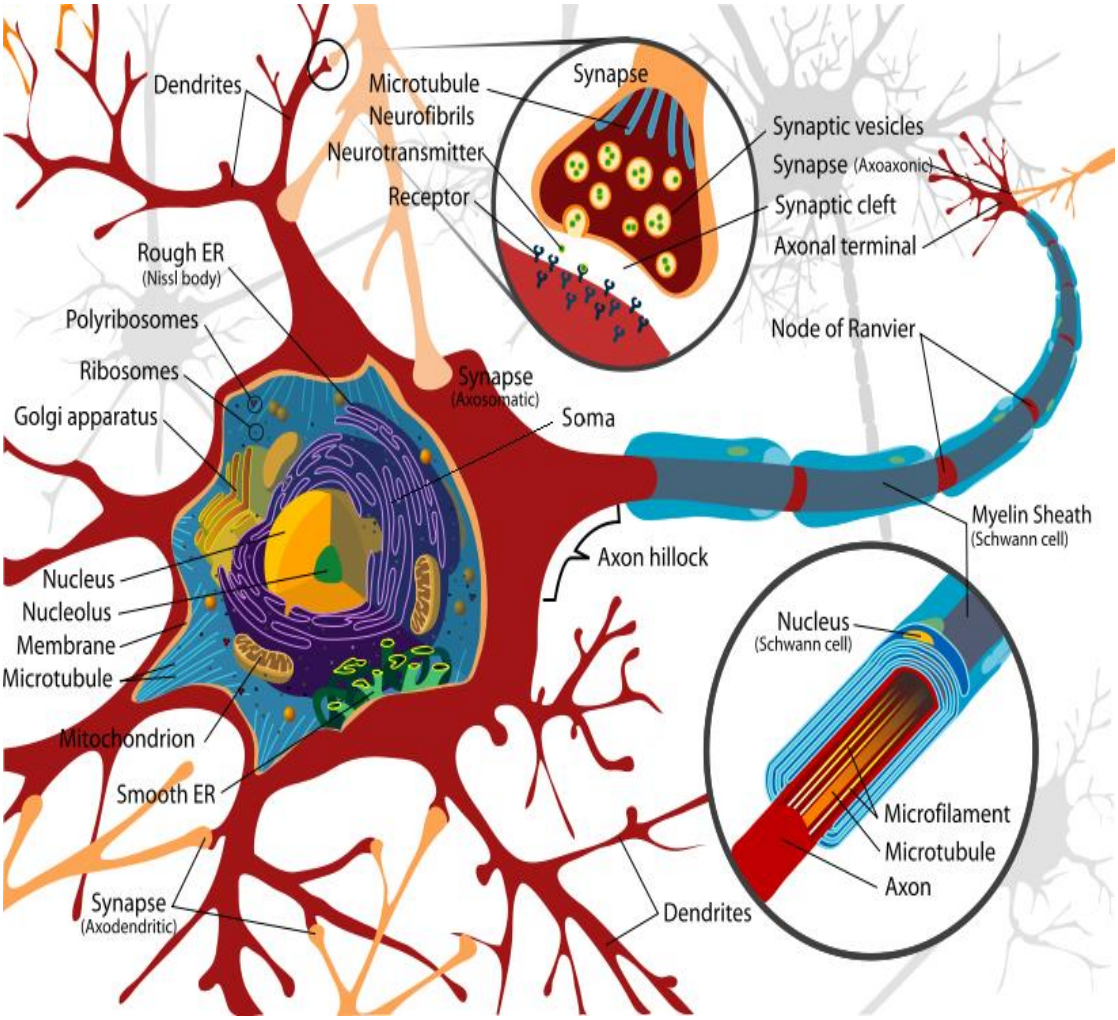


Figure 1: The schematic diagram of the neuron (M. R. Villarreal, 2007).

• The central part of the neuron is the soma. It houses the normal metabolic systems required to maintain the cell, such as nucleus, mitochondria and other organelles. All internal organelles are surrounded by a cell membrane and suspended in intracellular fluid, known as cytoplasm.

• The axon hillock connects the cell body to the axon. It contains the greatest density of voltage-dependent sodium channels. This makes it the most easily-excited part of the neuron and the spike initiation area for the axon.

• Some axons contain a fatty sheath around the axon called myelin, which provides electrical insulation for the covered sections of the axon membrane from the

extracellular fluid with the purpose of accelerating the propagation of an action potential along the axon. The areas between the consecutive myelin sections are the nodes of Ranvier, which cause regeneration of electrical signals.

Neuron is the most important concept in the brain. The estimated number of neuron in a human brain is from 80 to 120 billion neurons. In addition, neurons are unique because they can transmit electrical signals over long distances. The electric signal is transferred to the other neuron through the synapse in a chemical form or electric. Neuron received electrical signal from other neurons through dendrites.

It has a structure like a tree for increasing the ability of sensing the signal that comes from the other neuron through synapse connections and is sent to the body of the neuron that is called soma. The signal that is transmitted from the neuron came out through a special part called an axon to other cells as shown in Figure 2. Axon of the neuron length reaches a very long distance sometimes extending to the whole body.

In a mouse brain, the cortical neurons have been estimated that the length of axon is equal to about 40 mm and has in its branches almost 4 mm of total dendritic. Each axon makes connections of approximately 180 synaptic contacts per μm with other branches of dendritic that belong to other neurons. Also each dendritic tree receives an average of two signals per μm from another. The soma of ideal cortical neurons reaches in diameter from 10 up to 25 μm. (Abbot, 2002).

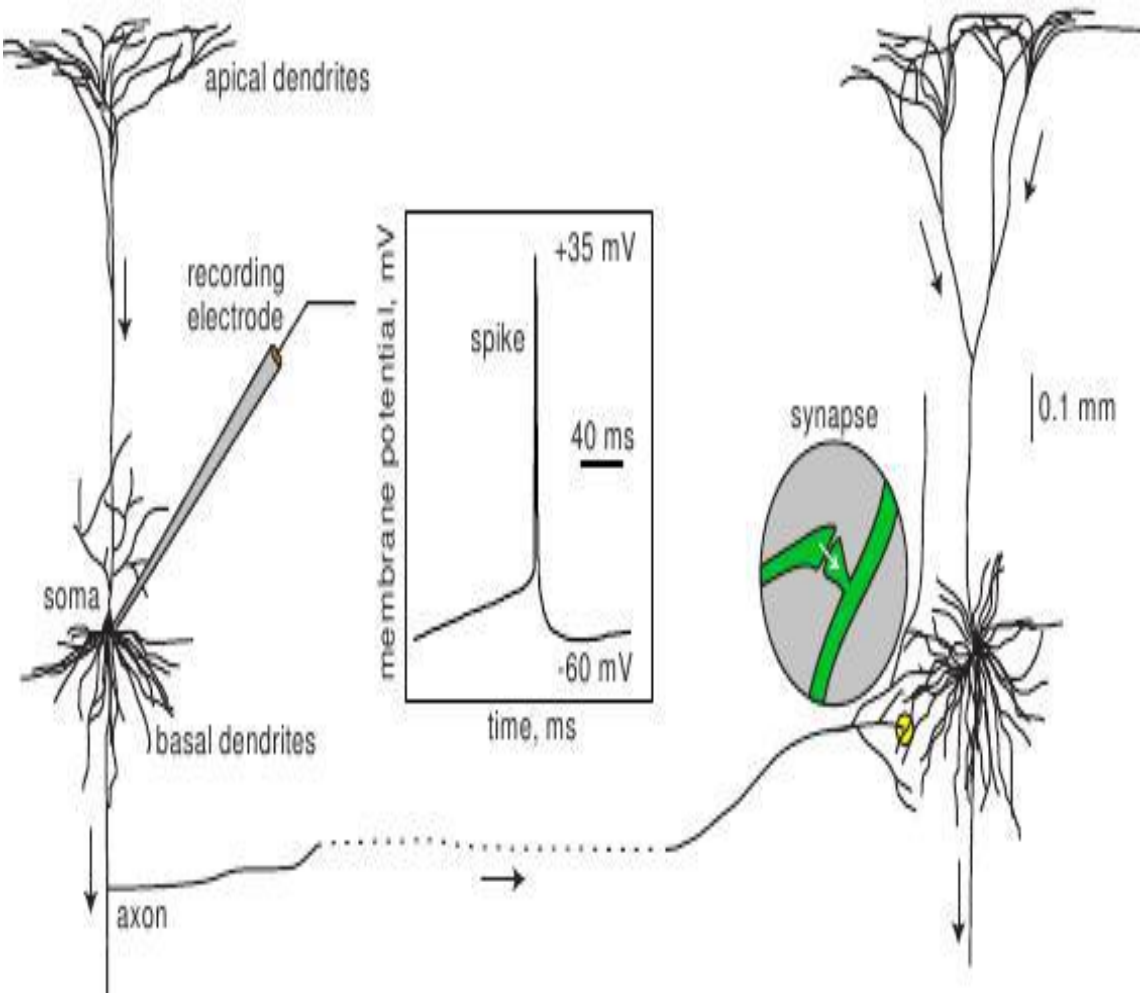


Figure 2: Two interconnected cortical pyramidal neurons and in vitro recorded spike (Izhikevich,2007).

### 2.1.1 What is a spike?

It is simply the communication means between the neurons. Each neuron received from 10 000 other via a dendritic tree which is synapse. Through a synapse from another neuron, electrical signal received causes the transmembrane current that changes the membrane potential (neuron voltage). The current signal that comes from the synapse is called the post synapse potentials (PSPs), little current generate tiny PSPs, large current means considerable PSPs. Voltage sensitive channel embedded in a neuron is amplified to result in generation of action potential or spike (Izhikevich, 2007).

### 2.1.2 Membrane proteins

Each neuron cell contains proteins specialized to transport materials through other. In order to understand many neurons functions some information about these proteins should be known. It could be classified into three groups according to how these proteins help to transport the substances in the membrane. Each type of protein's function has the ability to change its form according to that function.

#### 2.1.2.1 Channels

It is simply membrane protein that is made in a form of channel or hole, allowing some material to pass through. The size of the channel is varied according to the purpose of that channel so small sized holes control little sized substances to pass in or out into the cell and the same for different size of substances. There are protein molecules working as a channel like sodium (Na+), potassium (K+), calcium (Ca2+), and chloride (Cl-).

#### 2.1.2.2 Gates

One of the important protein's molecules features has special ability that can change its shape. These proteins are called gates. The purpose of the gates is to simply allow some or specific chemicals to pass and bind the others. These implanted proteins behave like a pass. It becomes active when the chemical match with the embedded proteins by the shape and the size, and there are many kinds of gate responses to different motivation such as electrical charge or temperature change to allow the certain chemical to pass through.

#### 2.1.2.3 Pump

It is the other type of membrane proteins that are modified to work as a pump, moving substances around the membrane according to the energy requirements for the transporter molecule. For example; proteins shaping their pattern in case to pump particular ions, ions like Na+ moving in one way and K+ ions in the opposite direction. Furthermore, protein pump transports many other substances.

### 2.1.3 Synapse

Synapse is designed in the form of a cross between two connected neurons. It exists in the end axon when the incoming axon is in contact with the out coming axon which belongs to the other neuron. Axons end at the synapse, when the electrical voltage created from the action potential making the ion channel to become open by generating the flow of Ca+2 that leads to release the neurotransmitter.

The neurotransmitter motivates the receivers or the postsynaptic side on the second neuron that the signal destination producing on that side ion-conducting making the channel open. The type of the ions flows on the synapse could cause an stimulative, depolarized, or an repressive, typically hyper-polarizing; depend on the postsynaptic neuron (Abbot, 2002).

Synapse is orderly scattered over the dendritic. Generally restrained synapse is more proximal than excitatory synapses. Although these two types are existed at distal dendritic area, and also when it's present at some spines in conjunction well followed by excitatory input (Segev I., 2003). In a lot of systems, the input source is already given (e.g. Pyramidal hippocampal cells and cerebellar Purkinje cells), and it is preferentially attached to its own dendritic tree region, instead of randomly scattered around the dendritic tree surface.

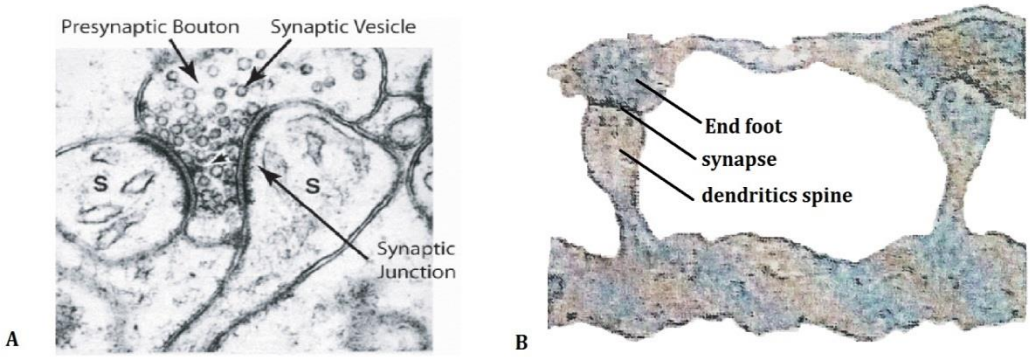


Figure 3: Synapses Examples (A) Electron micrograph of excitatory spiny synapses (s) shaped on the dendrites of a rodent hippocampal pyramidal cell. (B) An electron micrographic figure captured the synapse formed where the bottom terminal of one neuron meets a dendritic spine on a dendrite of another neuron (Kolb and Whishaw 2009).

## 2.2 Electrical activity of neuron and Membrane potential

The simple definition of membrane potential is the voltage potential or the difference of a neuron between the voltage measure inside the neuron, and the one measured outside the neuron.The potential that is created is considered as an equilibrium point because at this point the. In some conditions like resting state the voltage potential inside the neuron reaches about -70mV. However, this action potential is assumed conventionally to be zero mV for more fitness and also to consider the cell is polarized in this situation.The ions that will flow inside the cell should be equal in quantity to the ions moving outside the cell. The difference produced by this membrane potential is followed by keeping the concentration of an ion's gradient in balance, and this balance is controlled by the ion pumps placed in the cell. For instance, Na+ ions concentrated in the extracellular fluid is much longer than intracellular fluid, and also K+ ions in remarkable that is concentrated highly outside further than inside the neuron.

So the state transition of the neuron affected by the flow of ions from, and to the cell caused by voltage and concentration gradient. Positive charge ions produce current. These current flows out the neuron through open channels leaving negative charge in the membrane potential increased. This phenomenon is called hyperpolarization.The depolarization phenomenon happens when the current flows inside the cell making the membrane potential more negative or sometimes positive. When a neuron depolarizes enough to increase the level of the membrane potential higher than the threshold, a positive feedback operation starts and motivates the neuron to produce an action-potential, and the earlier reaches almost 100mV fluctuation in the electric potential through the cell membrane that is almost 1 millisecond last.

After action potential generates and is used to balance the potential between in and out the neuron, it may be leading to impossibility to start another spike after the depolarization making the neuron go to a period called the absolute refectory. The difference between the action potential and subthreshold fluctuation could be summarized by propagation over long distance.

In action, potential almost reaches 1 millimeter and the propagation of the signal without attenuation (Abbot, 2002). Figure 4 explains the dynamics of the voltage during an action potential during the synchronization by corresponding ions channel activities throughout an action potential. The resting potential in this figure represents the real value equal to -70mV.

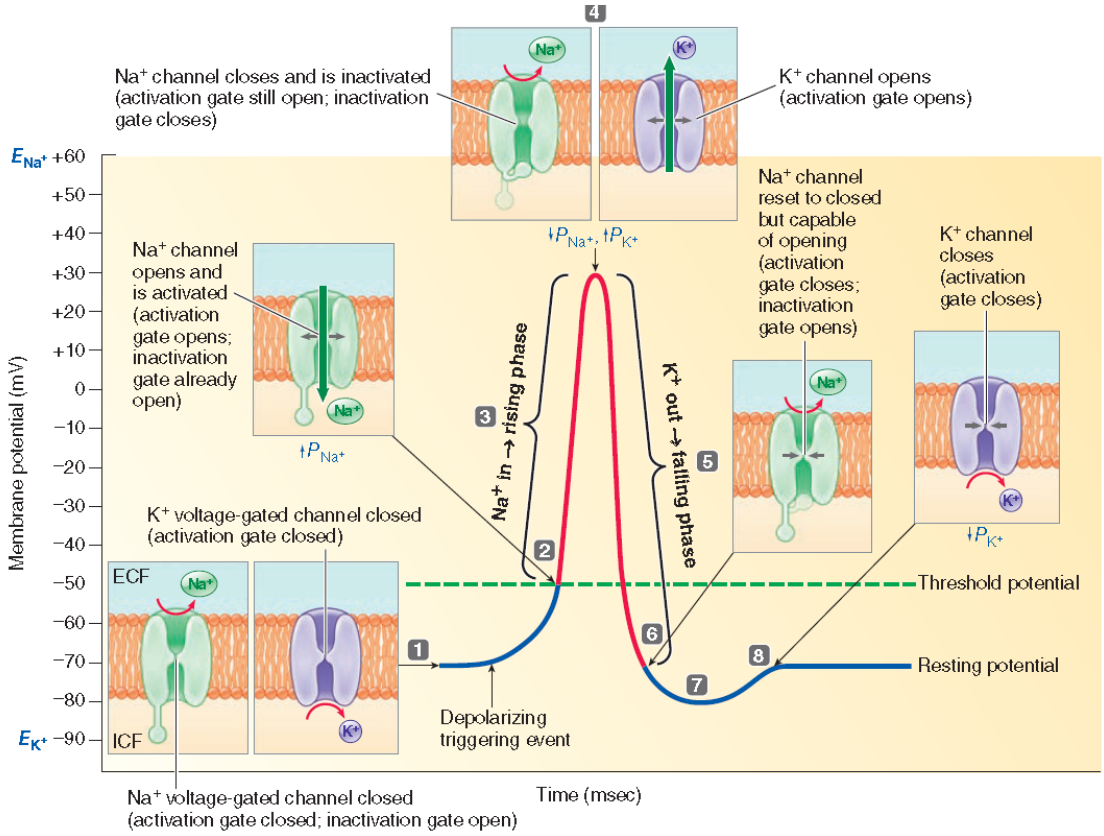


Figure 4: phase of action potential (Whishaw, 2012)

1- Resting potential: all voltage-gated channels closed.
2- At threshold, Na+ activation gate opens and P Na+ rises.
3- Na+ enters cell.
4- At peak of action potential.
5- K+ leaves cell.
6- On return to resting potential.
7- Further outward movement of K+ through still open K+ channel briefly hyperpolarizes membrane.
8- K+ activation gate closes, and membrane returns to resting potential.

The passage of an action potential can leave the ion channels in non-equilibrium state, making them more difficult to open, and thus inhibiting another action potential at the same spot (resting potential in Figure 5). Such a state is said to be refractory. The refractory period can be divided into two phases. In the first phase with a duration of about 1 ms to 5 ms, called the absolute refractory period, it is not possible for the neuron to fire another spike (i.e. the threshold is said to be infinite). In the second phase, called the relative refractory period with a length of 2 ms to 20 ms, the threshold slowly returns to its normal level. During this phase a spike could be emitted, but a stronger depolarisation of the membrane potential is required.

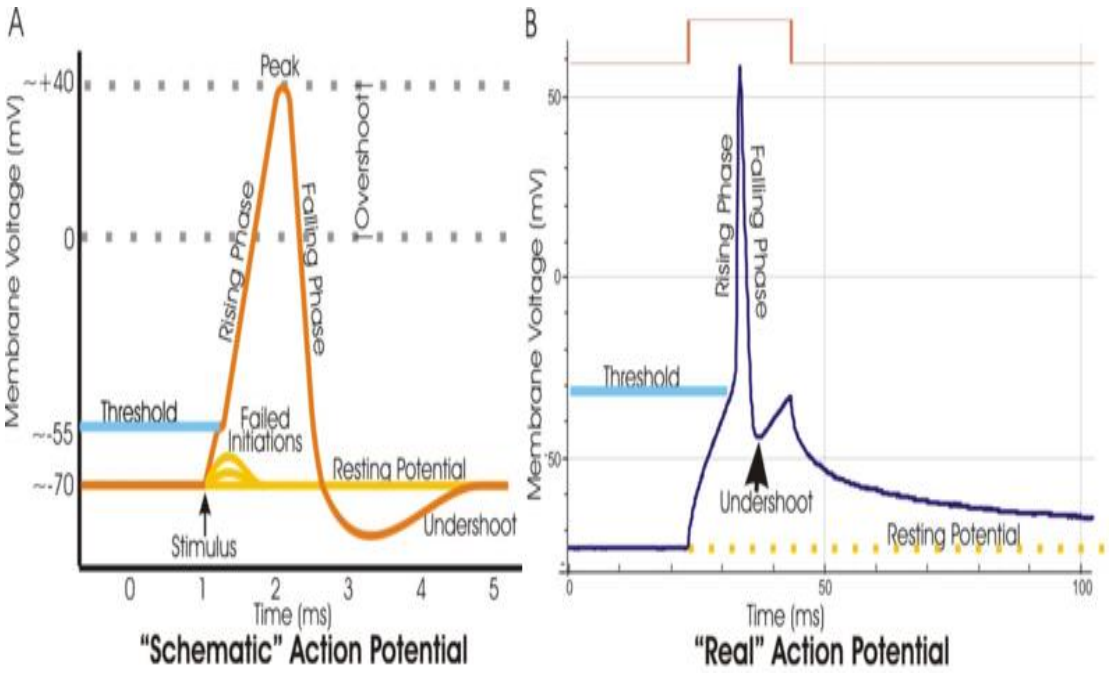


Figure 5: Schematic and real view of an action potential (G. Leonardo,2006).

### 2.2.1 Propagation

The triggered action potential propagates through the axon without fading out because the signal is regenerated at each patch of the membrane. Due to the myelin sheath the action potential travels further before being regenerated at the areas between the consecutive myelin sections known as the nodes of Ranvier, Figure 1. This accelerates the action potential propagation along the axon, since it only needs to be regenerated at the uncovered sections rather than continuously along the length of the axon. An action potential at one patch raises the voltage at nearby patches of the axon, depolarising them and provoking a new action potential there.

The diagram in Figure 6 shows a section of an axon, which is conducting an action potential. The action potential propagates through the axon and causes a back-propagation low amplitude pulse in the dendrites. a) The depolarized region on the far left causes sodium channels to open, further depolarising the region. b) At certain

point, the sodium channels become inactive and potassium channels open, which temporary depolarise the membrane. c) The process repeats as the wave of depolarisation propagates down the a. (G. J. Stuart and B. Sakmann,1994).

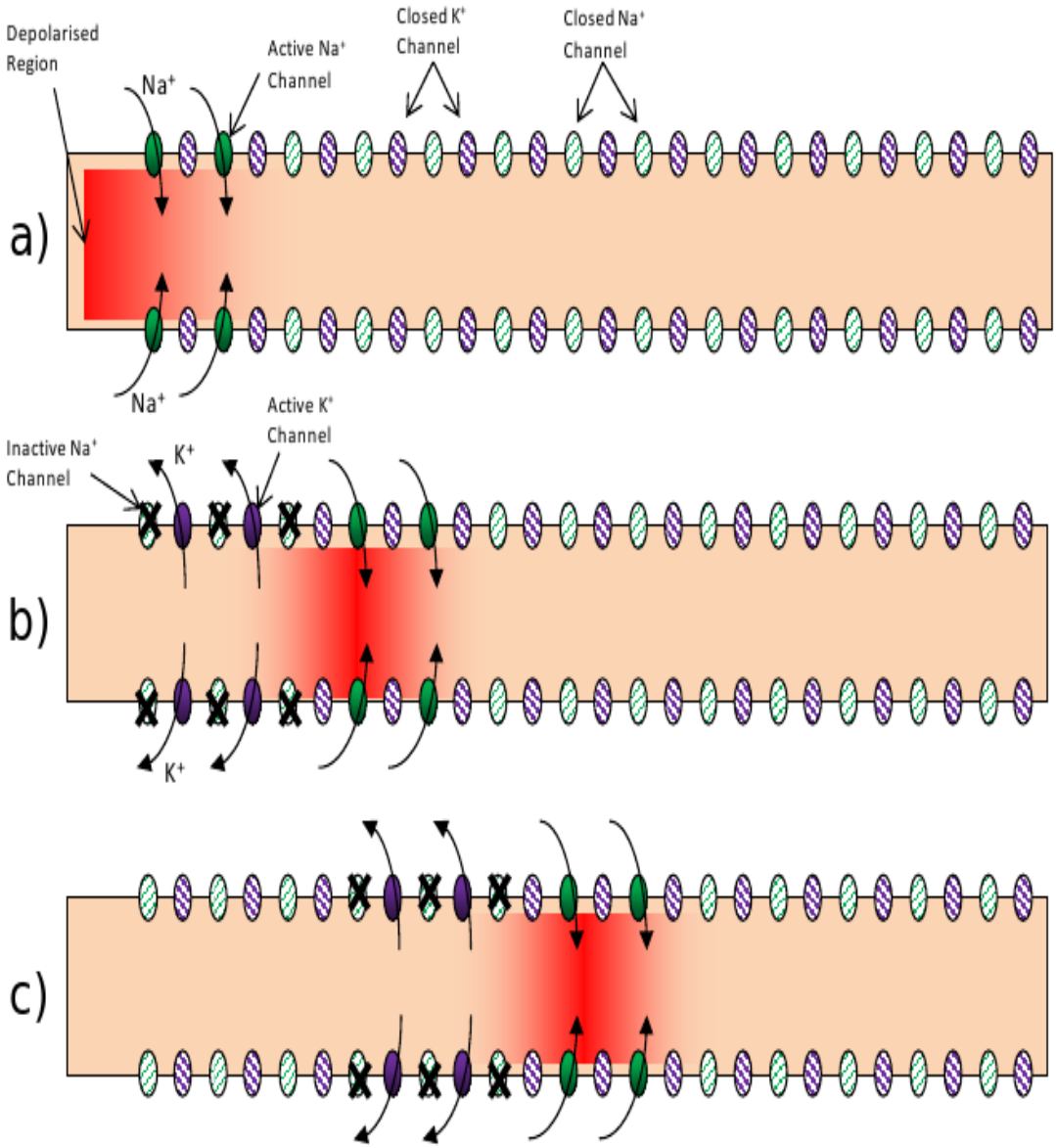


Figure 6: The propagation of an action potential (J. Bailey,2010).

# Chapter 3

# HODGKIN - HUXLEY EQUATIONS

In the last 60 years, a lot of neural models for different needs have been found and developed. Furthermore, the variety of these models relies on the structurally realistic biophysical model. For instance, one of the most important models through time is the Hodgkin – Huxley (HH), and the one that this thesis focus on the color noise model (set by Prof. Dr. Marifi Güler) which is, in fact, implementing the HH model to be more accurate if compared with the actual neuron.

Different models may be needed in various studies according to the biological properties of models, complication and the implementation cost. However, modeling technic of neural excitability has been attached from the monument work of Hodgkin-Huxley (1952). In this part the Hodgkin – Huxley model will be explained briefly.

## 3.1 The Hodgkin-Huxley Model

According to many investigations, experiment on giant squid axon by using clamp methods, Hodgkin and Huxley (1952) model show the current passing over the squid axon membrane composed of twain main ionic elements $I_{Na}$ (sodium channel current) and $I_K$ (potassium current). The membrane potential intensely dominated these two mentioned current.

As a consequence they developed a mathematical model of what they observe leading to create a model, until yet this model is mostly expressive model according to what many realistic neural models have been developed.

In the Hodgkin – Huxley model the electrical characteristics of a segment of nerve membrane could represented by an equivalent circuit in which current sources towards the membrane have two main parts; the first relative to charging membrane capacitance, the second is attached to the movement of special type of ions through the membrane. In addition, the ionic current composed of three different elements, a sodium current $I_{Na}$, a potassium current $I_K$ and a small leakage current $I_L$ usually it is related to chloride ions.

In 1952 Hodgkin and Huxley performed experiments on the axon of the giant squid and proposed a neuron model, derived from studies on the mechanisms responsible for generation of an action potential in a neuron. This neuron model is the most complex but also the most precise existing to date. It consists of four coupled differential equations expressing the dynamics of the membrane potential *Vm* of the neuron. This corresponds to the potential difference between the neuron and the

external environment. $V_m$ is a function of input current $I_{inject}$ applied to the neuron when it is stimulated, as shown in Figure 7. Currents $I_K$ and $I_{Na}$ are generated by the movement of K+ and Na+ ions through the membrane and the leakage current $I_L$, representing movements of Cl−. Each of these currents is based on the difference between the membrane potential Vm and the reversal potential $E_{Na}$, $E_K$ and $E_L$.

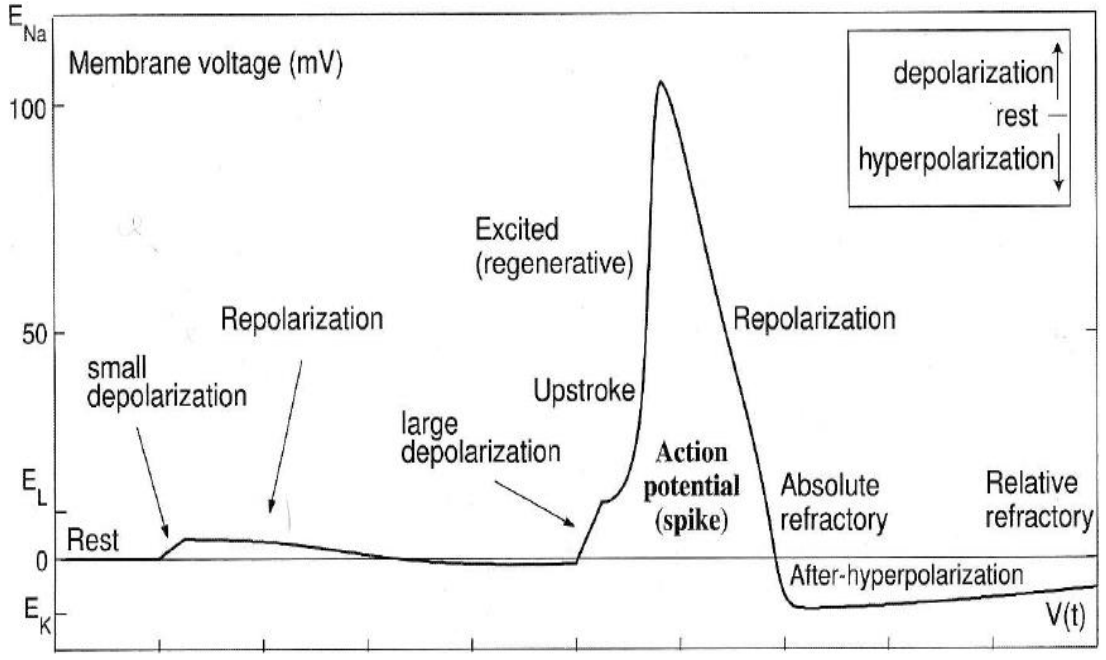


(a) Membrane potential.

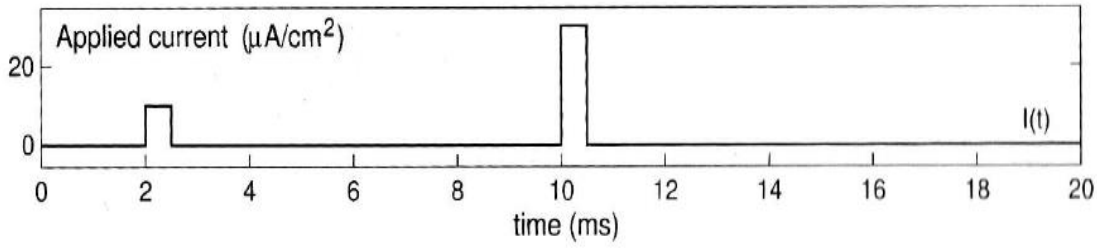


(b) Applied current.

Figure 7: Action potential generation in the Hodgkin-Huxley model (A. L. Hodgkin and A. F. Huxley,1952)

In the Hodgkin – Huxley model the electrical characteristics of a segment of nerve membrane could represented by an equivalent circuit in which current sources towards the membrane have two main parts; the first relative with charging membrane capacitance, the second is attached to the movement of special type of ions through the membrane. In addition, the ionic current composed from three different elements, a sodium current $I_{Na}$, a potassium current $I_K$ and a small leakage current $I_L$ usually it is related with chloride ions.

The differential equation similar to the electrical circuit is like follow

$$C_m \frac{dV_m}{dt} + I_{ion} = I_{ext} \quad (1)$$

Where $C_m$ is membrane capacitance, $V_m$ is membrane potential, and $I_{ext}$ is the current that externally applied. $I_{ion}$ is ionic current passing through the membrane and can be calculated from the next equation:

The $I_{ion}$ is the current influx onto the membrane and can be calculated from the following formulas:

$$I_{ion} = \sum_i I_i \quad (2)$$

$$I_i = g_i(V_m - E_i) \quad (3)$$

$I_i$ here demonstrate each single current having a relative conductance $g_i$ and reflex potential $E_i$

There are three $I_i$ in the squid giant axon model: sodium current $I_{Na,}$ potassium current $I_K$ and a small leakage current $I_L$ and the equation that represents those three currents is:

$$I_{ion} = I_{Na} + I_K + I_L \quad (4)$$

$$I_{Na} = g_{Na}(V_m - E_{na}) \quad (5)$$

$$I_K = g_K\,(V_m - E_K) \quad (6)$$

$$I_L = g_L\,(V_m - E_L) \quad (7)$$

The macroscopic $g_i(g_{Na}\ ,g_K\ ,\ g_L)$ Conductance's start from the united influence of a great amount of membrane microscopic ion channels. Ion channel can be considered as physical gates in a small number that manage the ions flow across the channel. When all the gates in an ion channel are in the permissive condition, ions can flow through the channel, and the channel is open.

### 3.1.1 The ionic conductance

In permissive state, all of the gates for a specific channel ion can go within a channel while the channel is open. The potassium and sodium conductance empirically described by the formal assumption, which is attained by voltage clamp experiments are:

$$g_k = \bar{g}_k n^4 \quad (8)$$

$$g_{na} = \bar{g}_{na} m^3 h \quad (9)$$

Where

$\left.\begin{matrix} \text{n} \\ \text{m} \\ \text{h} \end{matrix}\right\}$ Are ion channel gate variables dynamics

$\bar{g}_i$ is a constant with the dimensions of conductance per cm2 (mention that n between 0 and 1) . In order to normalize the result, a maximum value of conductance($\bar{g}_i$) is required.

The n, m, and h dynamic are listed bellow

$$\dot{\text{n}} = \frac{dn}{dt} = \alpha_n(1-n) - \beta_n n \tag{10}$$

$$\dot{\text{m}} = \frac{dn}{dt} = \alpha_m(1-m) - \beta_m m \tag{11}$$

$$\dot{\text{h}} = \frac{dh}{dt} = \alpha_h(1-h) - \beta_h h \tag{12}$$

$\alpha_x$ and $\beta_x$ are rate constant that the changes happened by voltage changes, but not affected with time, while the value of dimensions variable *n* can take place between 0 and 1, also it stand for of a single gate probability that is in permissive state.

The membrane potential in voltage clamp experiment begins in the resting period ($V_m$ = 0) and immediately reach to new clamp voltage $V_m = V_c$. the solution to the above equation (9) is by exponential of the form.

$$x(t) = x_\infty(V_c) - \big(x_\infty(V_c) - x_\infty(0)\big)\exp(-t/\tau_x) \quad (13)$$

$$x_\infty(0) = \alpha_x(0)/\alpha_x(0) + \beta_x(0) \quad (14)$$

$$x_\infty(V_c) = \alpha_x(V_c)/\alpha_x(V_c) + \beta_x(V_c) \quad (15)$$

$$\tau_x(V_c) = [\alpha_x(V_c) + \beta_x(V_c)]^{-1} \quad (16)$$

Where x represents time depending on gate variable n, m and h in order to make the formula easier the voltage value of gating variable has been assumed at resting state means the $x_\infty(0) = 0$ and $x_\infty(V_c) =$ the clamp voltage $V_c$. $\tau_x$ Represent the constant time required for reaching the steady state value of $x_\infty(V_c)$ when the voltage assumed equal to $V_c$. Hodgkin and Huxley measured constantly $\alpha_i$ $\beta_i$ as functions of *V* in the following

$$\alpha_i = \frac{x_\infty(V)}{\tau_n(V)} \quad (17)$$

$$\beta_i = \frac{1 - x_\infty(V)}{\tau_n(V)} \quad (18)$$

As discussed earlier before in the formula, i representing for n, m, and h ion channel gate. The coming equations are the formula.

$$\alpha_n(V) = \frac{0.01(10-V)}{\exp\left(\frac{10-V}{10}\right)-1}, \quad (19)$$

$$\beta_n(V) = 0.125 \exp\left(-\frac{V}{80}\right), \quad (20)$$

$$\alpha_m(V) = \frac{0.1(25-V)}{\exp\left(\frac{10-V}{10}\right)-1}, \quad (21)$$

$$\beta_m(V) = 4 \exp\left(-\frac{V}{18}\right), \quad (22)$$

$$\alpha_h(V) = 0.07 \exp\left(-\frac{V}{20}\right), \quad (23)$$

$$\beta_h(V) = \frac{1}{\exp\left(\frac{30-V}{10}\right)+1} \quad (24)$$

# Chapter 4

# DYNAMICS OF THE MEMBRANE

We consider the HH model throughout this study. Our analysis, however, is applicable to any conductance-based model with ion channels governed by linear, voltage-dependent kinetics. The membrane potential of a neuron is described by the equation:

$$C\ \frac{dV}{dt} = -g_K\ \psi_k\ (V_m - E_K) - g_{Na}\psi_{na}(V_m - E_{na}) - g_L(V_m - E_L) + I \qquad (25)$$

*V* above is the transmembrane voltage, and $\psi_K$ is the dynamic variable in the formula represents the ratio of open channel from potassium which is the proportional number of open channel to the complete number of potassium channel in the membrane; also $\psi_{Na}$ is open sodium channels ratio, and $I$ is externally current. All the constant parameters value of the membrane used in Eq. (25) is available in table below. All of the two channel variables $\psi_K$ and $\psi_{Na}$ in the Hodgkin–Huxley (HH) equations is taken as their approximated deterministic value, $\psi_K = n^4$ and $\psi_{Na} = m^3h$; while potassium channel have four n-gates and sodium channel have three m-gates and one h-gate. In case the channel is considered open, all the gates of that channel have to be open, and the gating variable for potassium is *n* and for sodium is *m* and *h*.

Table 1: Constants of the Membrane.

| $C$ | **Membrane capacitance** | **1µF/cm2** |
|---|---|---|
| $g_K$ | Maximal potassium conductance | 36mS/cm2 |
| $E_K$ | Potassium reversal potential | −12mV |
| $g_{Na}$ | Maximal sodium conductance | 120mS/cm2 |
| $E_{na}$ | Sodium reversal potential | 115mV |
| $g_L$ | Leakage conductance | 0.3mS/cm2 |
| $E_L$ | Leakage reversal potential | 10.6mV |
| | Density of potassium channels | 18 chns/µm2 |
| | Density of sodium channels | 60 chns/µm2 |

Thus, $N_K$ and $N_{Na}$ correspond to the complete numbers of channels for potassium and sodium. In order to get the total number of open channels, it should be simply multiplied the $N_K$ by 4n for potassium to get $4N_Kn$ and also for sodium resulting $3N_{Na}m$, $N_{Na}h$. On the other hand, the Markov process has been put into the gates dynamics. The probability of an n-gate is closed between the time t and still closed or becomes open at time t+Δt is exp $(-\alpha_n \Delta t)$, and the probability of being open at time $t$, and continue to be open at time $t + \Delta t$ is exp $(-\beta_n \Delta t)$ which means that all of the parameters $\alpha_n$ and $\beta_n$ are the rate of voltage-dependent opening and closing of n-gates. Also, the same process is applied for the m-gate and h-gate.

The rate functions that found to be as

$$\alpha_n = (0.1 - 0.01V)/(exp(1 - 0.1V) - 1), \quad (25a)$$

$$\beta_n = 0.125 \exp(-V/80), \quad (25b)$$

$$\alpha_m = (2.5 - 0.1V)/(exp(2.5 - 0.1V) - 1), \quad (25c)$$

$$\beta m = 4\, exp(-V/18), \quad (25d)$$

$$\alpha h = 0.07\, exp(-V/20), \quad (25e)$$

$$\beta h = 1/(exp(3 - 0.1V) + 1). \quad (25f)$$

## 4.1 NCCP [The non-trivial cross correlation persistency]

As pointed out earlier, in the potassium channel there is more than one n-gate and even if the proportions of open gates are known, it is not enough to satisfy $\psi_K$. Take for instance a membrane to consist of pair of potassium channels (eight gates), probably in case of at time $t_2$, it can be noticed that one of the two channels has all its gates open while the other channel only has two open gates. However, in a different time period of time $t_1$, each of the channel has the same number of open gates, which means even that membrane has equal number of open gates during the two periods of time, one of the two channel is open in moment $t_2$ but there is no channel at moment $t_1$ (see Figure 8) although the term *gate-to-channel uncertainty* specifies this disadvantage of knowledge that is placed in $\psi_K$ and even if *n* is known and also the expression *gate noise* is significant in these random fluctuations in *n* (Güler, 2011).

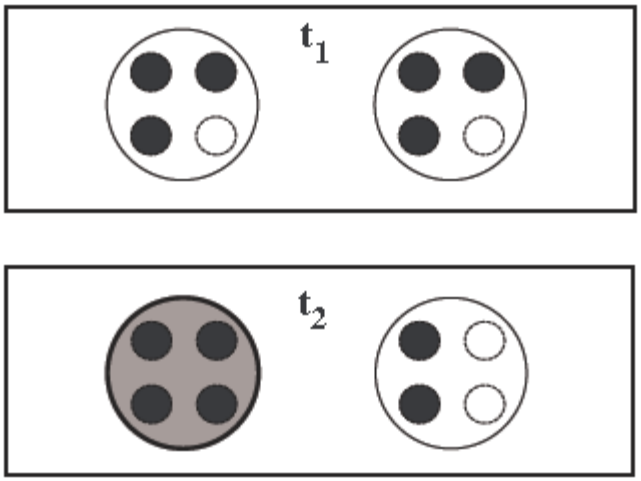


Figure 8: the toy membrane at two possible conformational (Güler, 2011).

The gate-to-channel is considered as dynamic random fluctuations in the construct $\psi_K - [\psi_K]$, by this construct the channel fluctuations that appear from the *gate-to-channel uncertainty* is bounded. If the *gate-to-channel uncertainty* did not exist, the construct could be disappearing regardless of the gate noise. Here $[\psi_K]$ is framed for the arrangement mean of the ratio of open potassium channels; calculated through all achievable arrangement of the membrane getting $4NKn$ open n - gates, as shown below.

$$[\psi K] = \begin{cases} \frac{(4N_K n-3)(4N_K n-2)(4N_K n-1)n}{(4N_K-3)(4N_K-2)(4N_K-1)}, if\ N_{K^n} \geq 1 \\ o \qquad\qquad\qquad\qquad , \quad otherwise \end{cases} \tag{26}$$

Then the construct $\psi_K - [\psi_K]$ will evaluate the difference between number of open channels from the arrangement mean at any moment. Except if the membrane is very small in size, it will be $[\psi_K] \approx n^4$. In case of finite membrane but unlimited in size, the construct fluctuations will disappear. Thus, when membranes are large, the HH value to be used is $\psi_K = [\psi_K] = n^4$ at any time. The construct could be irrelevant in

another condition when each of the channels has only one gate open, whatever the membrane size was, so actually we will have $\psi_K = [\psi_K] = n$ .

Definition of the order parameters $\Omega_K^V$ and $\Omega_K^n$ as the given cross correlations will be:

$$\Omega_K^V = \frac{((\psi_K - [\psi_K])V) - (\psi_K - [\psi_K](V)}{([\psi_K])(E_{Na} - E_K)} \tag{27}$$

$$\Omega_K^n = \frac{((\psi_K - [\psi_K])n) - (\psi_K - [\psi_K](n)}{([\psi_K])(n)} \tag{28}$$

Here the expectation values $< \cdot >$ are simply the foundation averages above the membrane conformation condition and all of these conformation conditions are related to time. Separately from each other's, through using Markovian process of the consisting gate condition and in Equation (25); the ensemble during $t + \Delta t$ is set from the starting moment $t$, to satisfy suitability of the scale and the dimensionality these terms are included. $\Omega_k^v$ Represent the evaluation for correlation among the voltage fluctuations $V$ and the fluctuations of the construct $\psi_K - [\psi_K]$. $\Omega_k^n$ is almost the same, controlling the fluctuations of $n$ instead of $V$. This is due to the fact that the construct positivity or negativity is going completely irregular and uncontrollable by any of the fluctuations of $V$ or $n$. After an initial passing moment becomes easy to predict that the order parameters decrease to none and this initiation is wrong in both the theoretical arguments and the numerical experiments of the channels. However, according to the simulations for near-equilibrium dynamics, the order parameter becomes and continues less than zero within the phase of sub-threshold actions. A non-trivially continual correlation reserves a position between the fluctuations of V and the fluctuations of the construct $\psi_K - [\psi_K]$ and also the fluctuations of n, and this phenomenon what NCCP is pointing on.

It is passable that the order parameters remain not zero as specified in Markovian evaluation that the condition of the gate at moment t + Δt is relied on condition at moment t: even through the degree of dependence declining with the time period in Δt becoming larger. This means that the construct $\psi_K - [\psi_K]$ has not got a disappearing autocorrelation function and the time of the autocorrelation is limited, not reaching to zero. Thus, leading the plus value of [V − EK] becomes useful and it can be removed from the equation (18) in the condition that $\psi_K - [\psi_K]$ is greater than zero during some amount of time, after that a negative variance appearing in dV/dt along with that period. At this point, the variance is depending on having the construct $\psi_K - [\psi_K]$ equal to zero in the same duration, and from that the variance turns to negative in that period. That property is portrayed by

$$\psi_k - [\psi_k] > 0 \Rightarrow \delta\left(\frac{dV}{dt}\right) < 0 \Rightarrow \delta V < 0 \tag{29}$$

Likewise, the variation in the situation of negative $\psi_K - [\psi_K]$ was shown as

$$\psi_k - [\psi_k] < 0 \Rightarrow \delta\left(\frac{dV}{dt}\right) > 0 \Rightarrow \delta V > 0 \tag{30}$$

In the two above equations, (27) and (28), if the sign of $\psi_K - [\psi_K]$ is not considered, the value of $(\psi_K - [\psi_K])\delta V$ is minus during the all-time passing out making $\psi_K - [\psi_K]$ not going to a positive. A graphical demonstration shown in Figure 9 in case that the dwelling time of $\psi_k - [\psi_k]$ in the same of algebraic sign should not be less than the duration of an actual fluctuation in V.

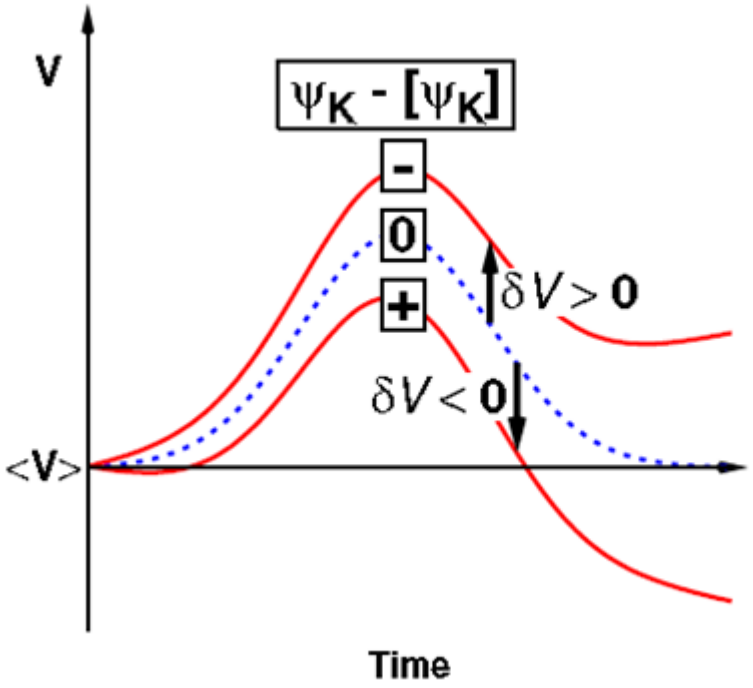


Figure 9: explanation in the diversity of the voltage V (Güler, 2011).

Furthermore, if the sign of the product $\psi_K - [\psi_K]$ is switched at some point in the period, the value of the previous will not become below zero again at any moment; for a short moment straight after the sign turned leading to change the sign to positive. In case of that the dwelling period is assumed remarkably higher than the repose time of the $\psi_K - [\psi_K]$ to become below zero again, the chances of the output in negative will be bigger than finding the product in positive. As a result, the voltage fluctuations V will be negatively correlated with the fluctuations of $\psi_K - [\psi_K]$. Therefore, the configuration variable $\Omega_k^v$ will reach minus value. The fluctuations, long-lasting only at a microscopic time window, enforce order at macroscopic time window.

In addition, one of the reason that the order parameter $\Omega_k^n$values does not become zero, is that the deference of variation δV from V, with the deviations from $\psi_K - [\psi_K] = 0$. All of the rates $\alpha_n$ and $\beta_n$are a voltage relevance function that increases with the voltage. Since a rise in $\alpha_n$ decreases the expectation of a closed n-gate staying closed and a reduction in $\beta_n$increases the chances of an open n-gate to be open, a positive δV is producing a positive change in the gating inconstant n. This progress, similar to $\Omega_k^v$, $\Omega_k^n$ also achieves a negative value.

## 4.2 The relationship between NCCP and the sodium channels

The concept that displays the gate-to-channel uncertainty linked with the sodium channels is $\psi_{Na} - [\psi_{Na}]$. At this point, the structure medium of the ratio of open sodium channels, $[\psi_{Na}]$, becomes.

$$[\psi K] = \begin{cases} \frac{(3N_{Na}m-2)(3N_{Na}m-1)m}{(3N_{Na}-2)(3N_{Na}-1)}, if\ N_{Na}m \geq 1 \\ o \qquad\qquad\qquad\quad , otherwise \end{cases} \tag{31}$$

Only if the membrane is very tiny in size, to considered as

$$[\psi_{\mathrm{Na}}] \approx m^3 h \tag{32}$$

When we have a set membrane with infinite size, the HH value $\psi_{Na} = [\psi_{Na}] = m^3 h$ assigns at all times. The main order variable of relate to the sodium channels, $\Omega_{na}^v$, is provided by.

$$\Omega_{Na}^V = \frac{((\psi_K - [\psi_{Na}])V) - ((\psi_{Na} - [\psi_{Na}](V))}{([\psi_{Na}])(E_{Na} - E_K)} \tag{33}$$

The simulations showing that $\Omega_{na}^{v}$ gets positive values and constantly is still in positive, within the phase of sub-threshold action. This is only for the near-equilibrium dynamics, a non-trivially continual correlation gets placed amongst the fluctuations of the construct $\psi_{Na} - [\psi_{Na}]$ and the changes of V remarking that the sign of $\Omega_{na}^{v}$ is conflicting with the sign of $\Omega_{k}^{v}$. It is because of the signs of $V - E_k$ and $V - E_{na}$ in Equation (25) are opposite at any moment, the previous is positive and the final is negative

## 4.3 Major Impact of NCCP

It was expected that the increases in the diversity of the amplitude of sub-threshold voltage fluctuations are caused by the NCCP, which is through increasing the probability of fluctuations with bigger amplitudes which is covered in depth in Güler, 2013. After that, it was demonstrated that the diversity in making easier for the cell's spiking through forcing the passing from the firing to the sub-threshold phase has become simpler. On the other hand, it was found that limited scale membranes beholden their upraised irritability not only to the gate noise but, to a larger range, as well as to NCCP. Furthermore, NCCP was noticed to improve the consistency in spiking.

# Chapter 5

# THE GULER MODEL

The colored stochastic Hodgkin Huxley equations (Güler, 2013) are given by:

$$C\dot{V} = -g_k\psi_K(V - E_K) - g_{Na}\psi_{Na}(V - E_{Na}) - g_L(V - E_L) + I \tag{34}$$

$$\psi_K = n^4 + \sqrt{\frac{n^4(1-n^4)}{N_K}}q_K \tag{35}$$

$\psi_k$, is the gates variable for potassium channel.

$$\psi_{Na} = m^3h + \sqrt{\frac{m^3(1-n^4)}{N_{Na}}hq_{Na}} \tag{36}$$

$\psi_{na}$, is the gates variable for sodium channel.

$q_K$ and $q_{Na}$, are a stochastic variable with zero expectation value at equilibrium and has some autocorrelation time greater than zero. The equations that describe the dynamics of $q_K$ are specified accordingly as follows:

$$\tau\dot{q_K} = p_K \tag{37}$$

$$\tau \dot{p_K} = -\gamma_K p_K - w_K^2[\alpha_n(1-n) + \beta_n n] g_K + \xi_K \quad (38)$$

The equations that describe the dynamics of $q_{Na}$ are specified accordingly as follows:

$$\tau \dot{q}_{Na} = p_{Na} \quad (39)$$

$$\tau \dot{p}_{Na} = -\gamma_{Na} p_{Na} - w_{Na}^2[\alpha_m(1-m) + \beta_m m] g_{Na} + \xi_{Na} \quad (40)$$

The parameter $\tau$ corresponds to the unit time. The constants $\gamma_K, \gamma_{Na}, w_K^2, w_{Na}^2$ and the variables $q_K, q_{Na}$ and $p_K, p_{Na}$ are all in dimensionless units.

A complete set of analytic activity equations must capture not only NCCP but also the gate noise.

$$\dot{n} = \frac{dn}{dt} = \alpha_n(1-n) - \beta_n n + \eta_n \quad (41)$$

$$\dot{m} = \frac{dn}{dt} = \alpha_m(1-m) - \beta_m m + \eta_m \quad (42)$$

$$\dot{h} = \frac{dh}{dt} = \alpha_h(1-h) - \beta_h h + \eta_h \quad (43)$$

Where the Gaussian white-noise terms have zero means, and their mean squares obey.

$$\langle \xi_K(t) \xi_K(t') \rangle = \gamma_K T_K[\alpha_n(1-n) + \beta_n n] \delta(t-t') \quad (44)$$

$$\langle \xi_{Na}(t)\xi_{Na}(t') \rangle = \gamma_{Na} T_{Na}[\alpha_m(1-m) + \beta_m m]\delta(t-t') \quad (45)$$

$$\langle \eta_n(t)\eta_n(t') \rangle = \frac{\alpha_n(1-n)+\beta_n n}{4N_K}\delta(t-t') \quad (46)$$

$$\langle \eta_m(t)\eta_m(t') \rangle = \frac{\alpha_m(1-m)+\beta_m m}{3N_{Na}}\delta(t-t') \quad (47)$$

$$\langle \eta_h(t)\eta_h(t') \rangle = \frac{\alpha_h(1-h)+\beta_h h}{N_{Na}}\delta(t-t') \quad (48)$$

When the membrane size limits of infinite, it can be observed that the set of equation shrink to the HH equations. The constant parameters in the model were not appraised analytically. The values of the parameters were estimated by phenomenological methods through numerical experiments, as given in table 2. It was concluded that the dynamics forced by the equation in not reactive to the constant parameter values.

The colored noise terms in eq. (35) and eq. (36) serve the purpose of capturing NCCP. The white terms in eq. (41) - (43) correspond to gate noise.

Table 2: Constant Parameters of the Models

| | | |
|---|---|---|
| $\gamma_K = 10$ | $\omega^2{}_k = 150$ | $T_k = 400$ |
| $\gamma_{Na} = 10$ | $\omega^2{}_{Na} = 200$ | $T_{Na} = 800$ |

## 5.1 Noise (GWN)

Gaussian white noise process with zero mean and unit variance. This type of input is commonly used to characterize the response of stochastic Hodgkin-Huxley models (Rowat P. Neural Comput. 2007, Sengupta B. 2010), The additive white noise term can be interpreted as a simplified method for representing the combined effect of numerous synaptic inputs that neurons in cortex and other networks receive in vivo;, ( Abbott LF. Phys Rev Lett. 2001), and Gaussian noise is statistical noise that has its probability density function equal to that of the normal distribution, which is also known as the Gaussian distribution. In other words, the values that the noise can take on are Gaussian-distributed. A special case is white Gaussian noise, in which the values at any pairs of times are statistically independent (and uncorrelated). In applications, Gaussian noise is most commonly used as additive white noise to yield additive white Gaussian noise.

Noise can have a significant impact on the response dynamics of a nonlinear system. For neurons, the primary source of noise comes from background synaptic input activity. If this is approximated as white noise, the amplitude of the modulation of the firing rate in response to an input current oscillating at frequency omega decreases as 1/square root[omega] and lags the input by 45 degrees in phase. However, if filtering due to realistic synaptic dynamics is included, the firing rate is modulated by a finite amount even in the limit omega-->infinity and the phase lag is eliminated.

Thus, through its effect on noise inputs, realistic synaptic dynamics can ensure unlagged neuronal responses to high-frequency inputs.

When the classical Hodgkin-Huxley equations are simulated with Na- and K-channel noise and constant applied current, the distribution of interspike intervals is bimodal: one part is an exponential tail, as often assumed, while the other is a narrow gaussian peak centered at a short interspike interval value.

The gaussian arises from bursts of spikes in the gamma-frequency range, the tail from the interburst intervals, giving overall an extraordinarily high coefficient of variation--up to 2.5 for 180,000 Na channels when I approximately 7 microA/cm. Since neurons with a bimodal ISI distribution are common, it may be a useful model for any neuron with class 2 firing. The underlying mechanism is due to a subcritical Hopf bifurcation, together with a switching region in phase-space where a fixed point is very close to a system limit cycle. This mechanism may be present in many different classes of neurons and may contribute to widely observed highly irregular neural spiking.

The stochastic opening and closing of voltage-gated ion channels produce noise in neurons. The effect of this noise on the neuronal performance has been modeled using either an approximate or Langevin model based on stochastic differential equations or an exact model based on a Markov process model of channel gating. Yet whether the Langevin model accurately reproduces the channel noise produced by the Markov model remains unclear.

## 5.2 Spike coherence

A sensitively regular measure of spike train is called coefficient of variation (CV), or the comparative difference of the interspike interval distribution. This regularity measure is given by,

$$CV := \frac{\sqrt{\langle T^2\rangle - \langle T\rangle^2}}{\langle T\rangle}. \tag{49}$$

$\langle T\rangle$: The mean interspike interval is given by this formula $\langle T\rangle = \lim_{N\to\infty} \frac{1}{N}\sum_i T_i$.

$\langle T^2\rangle$: The mean squared interval $\langle T^2\rangle := \lim_{N\to\infty} \sum(t_{i+1} - t_i)^2/N$.

CV = 1 if the sequence of spikes, which corresponds to the Poissonian spike train, is discrete.

CV<1 if the spike train are more ordered.

CV=0 for a purely deterministic response.

The increasing system size A is against to the coefficient of variation. While the firing rate reduces monotonically with regard to the patch area, it has been proved that the coefficient of variation (CV) shows a discriminate minimum for an optimal patch size for which the spike train is mostly regular at same value.

The phenomenon is called an intrinsic coherence resonance (Schmid &Hanggi, 2001). At optimal dosage of internal noise, whose optimal size of the cell membrane patch approximately $A = 1\mu m^2$, the CV shows a minimum, where the spiking becomes prevalently more ordered. The external disturbances withstand by internal rhythm which is possessed through the spiking activity (Schmid &Hanggi, 2007).

# Chapter 6

# RESULT AND DISCUSSION

This section consists on the series of experiments that actually defined efficiency of the colored noise by comparing colored noise model with the microscopic simulations. For this purpose, simple stochastic method has been used as the microscopic simulation scheme (Zeng, 2004).

This method was simply applied to the Markovian process to simulate each gate individually and keep continue for the rest of the gates. Noise variation in this simulation was a periodic sin wave under noise variance, as shown below:

$$I(t)= I_{base} +\xi(t) \tag{50}$$

Here, $I_{base}$ indicates the current situation, while $\xi(t)$ is Gaussian white noise with the mean zero. A series of experiments have been used to examine the effectiveness of the colored noise model in a comparative manner with the Microscopic simulation, as mentioned above. Firstly, by running experiments without including the colored noise model into the stochastic of the Hodgkin Huxley equations, and secondly by applying experiments again with the same parameters, but at this time the colored noise model was also included in stochastic of HH equations, as described in formula (50).

Thus, whatever figures have been driven out as a result (10, 11, 12, 13, 14, 15, 16, 17), there is a difference between the spike frequency of the HH equations without color noise and HH equation stochastic with colored noise, which is actually containing the spikes from microscopic simulation. As discussed earlier, NCCP affects are associated behind this driven difference, but when the noise variance increases the difference between spike frequencies becomes smaller even till it disappeared.

From the above experiments' result, it can also be analyzed that the mean spiking rates against the noise variances are displayed by a different membrane patch, that are actually comprised of (150, 300, 600, 900, 1800, and 2700) potassium channels, (1000, 2000, 3000, 6000, 9000) sodium channels with different $I_{base}$ (0, 2, 4, 6, -2, -4, 20, 100) and with different noise variance (0, 0.5, 1, 1.7, 2, 2.1, 2.9, 3, 3.6, 4, 4.8, 5, 6, 7, 8, 9, 10, 12, 14, 16,18, 20, 22, 24, 30, 36, 38, 40). Hence, it can be seen that the performance of colored noise was quite similar to the microscopic simulations.

Meanwhile, in consequent figures (18, 19, 20, 21), coefficient of variation with diverse membrane patches specifically comprised of (300, 900, 1800, 2700 and 3210) potassium channels, (1000, 3000, 6000, 9000 and 10700) sodium channels with different $I_{base}$ (0, 2, 4, 6, 8) and with several noise variances (2, 4, 6, 8, 10, 12, 14) has been calculated. A compute of the spike coherence is the coefficient of variation given by the formula (49). In above results it is clear that at the very beginning there is difference in spikes' frequencies, but when there is an addition in noise variance mostly around (4, 6 and 8), the coefficient of variation of the microscopic simulation with the stochastic HH equation and the colored term is getting smaller.

## Technologies Used

A computer program that solves the model eqns. (35, 36) numerically was developed by Güler. In the program, the input current was time independent which was modified so that the program could handle time dependent current. The model was developed by using C++ programing language and MATLAB was used for plotting the result.

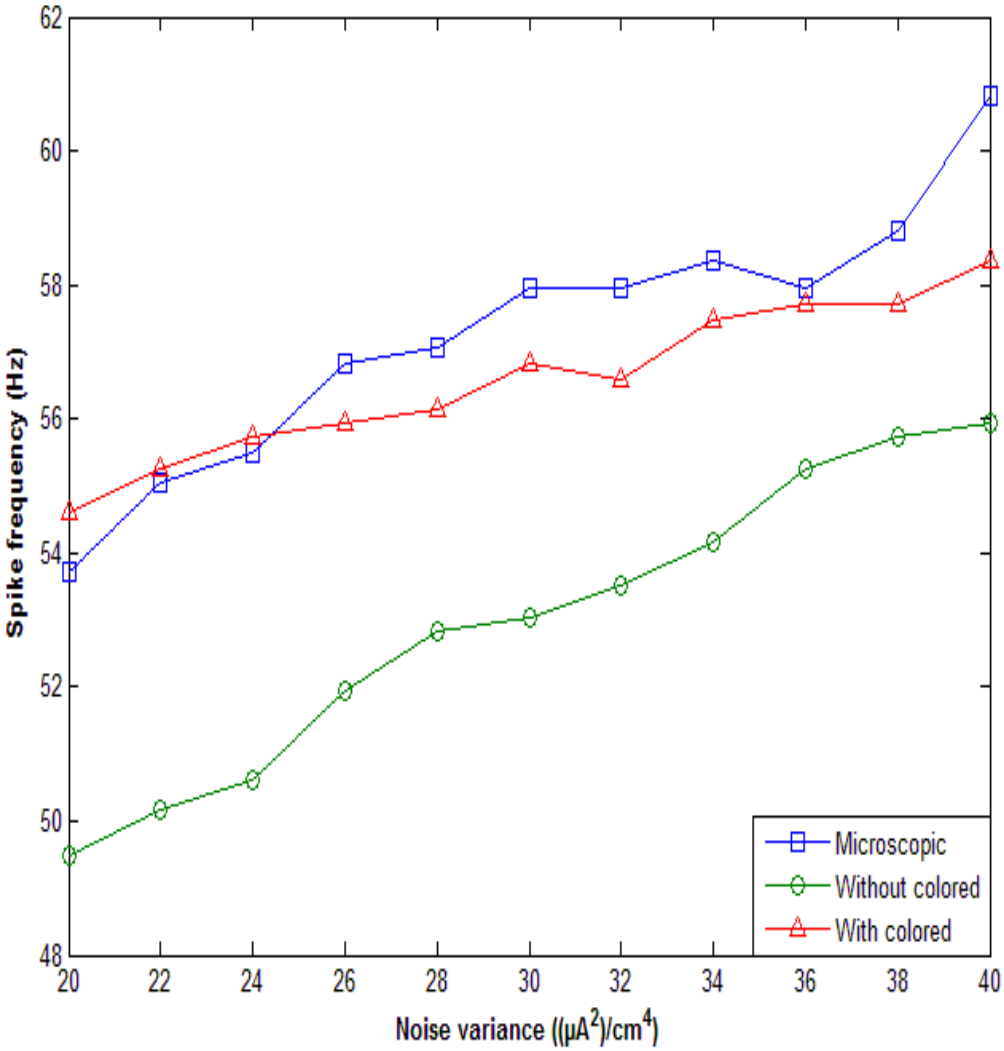


Figure 10: Mean spiking rates against the noise variance. The three curves represent the comparison between the microscopic simulation and the Güler model with colored noise and without colored noise terms. The membrane size for potassium is 300, for sodium is 1000 and $I_{base}$ = 2, in 5 seconds time window.

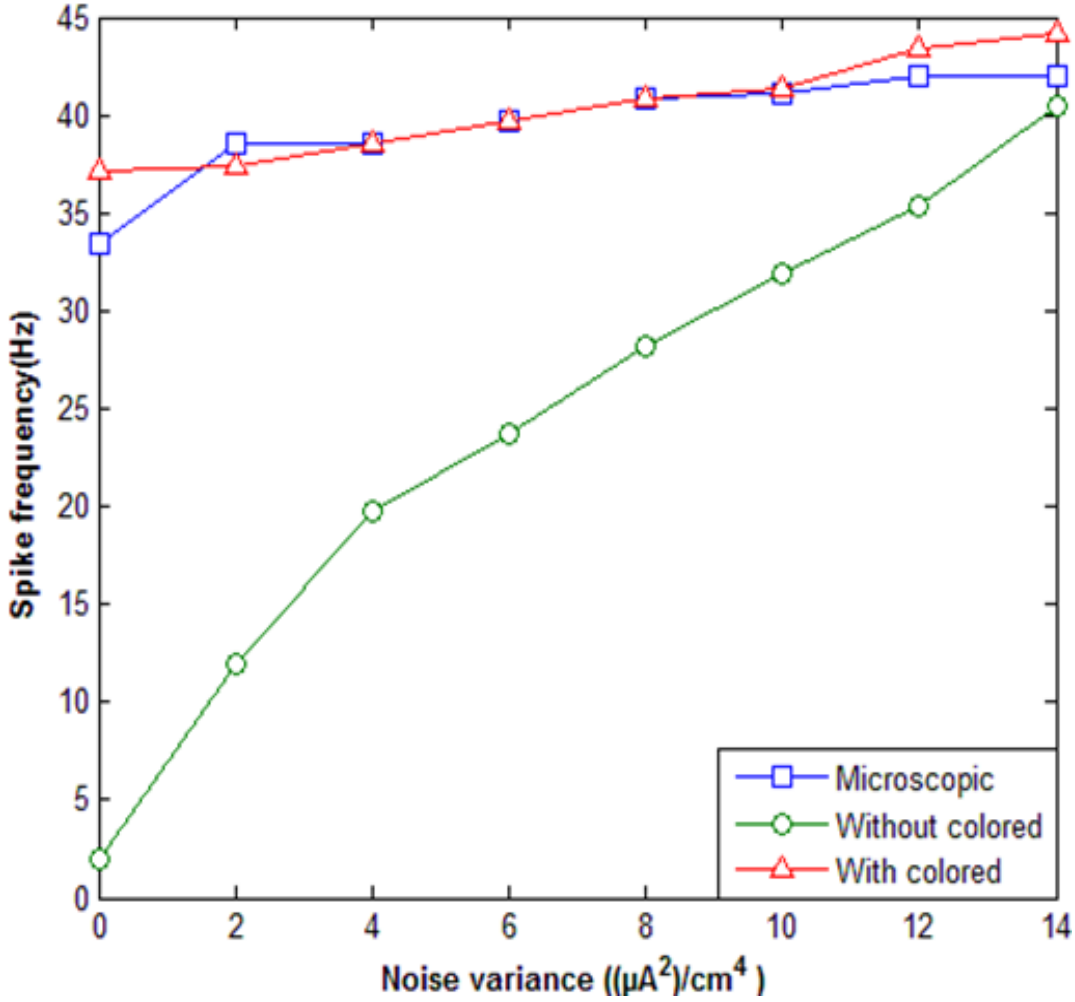


Figure 11: Mean spiking rates against the noise variance. The three curves represent the comparison between the microscopic simulation and the Güler model with colored noise and without colored noise terms. The membrane size for potassium is 300, for sodium is 1000 and $I_{base}$ = 0, in 5 seconds time window.

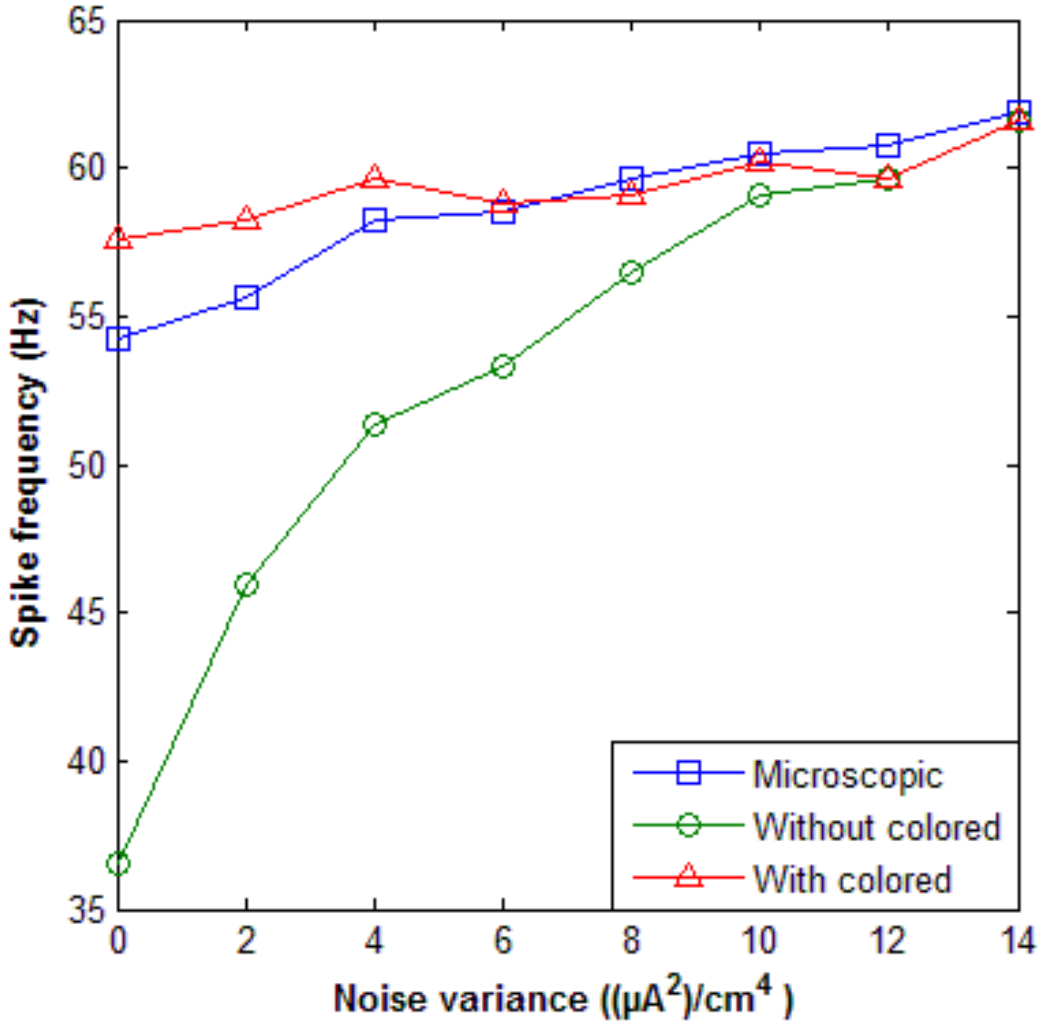


Figure 12: Showing in this figure the membrane size for potassium is 900 and for sodium is 3,000, $I_{base}$ =6. In addition, the three curves represent the comparison between the microscopic simulation and the Güler model with colored noise and without colored noise terms , in 5 seconds time window.

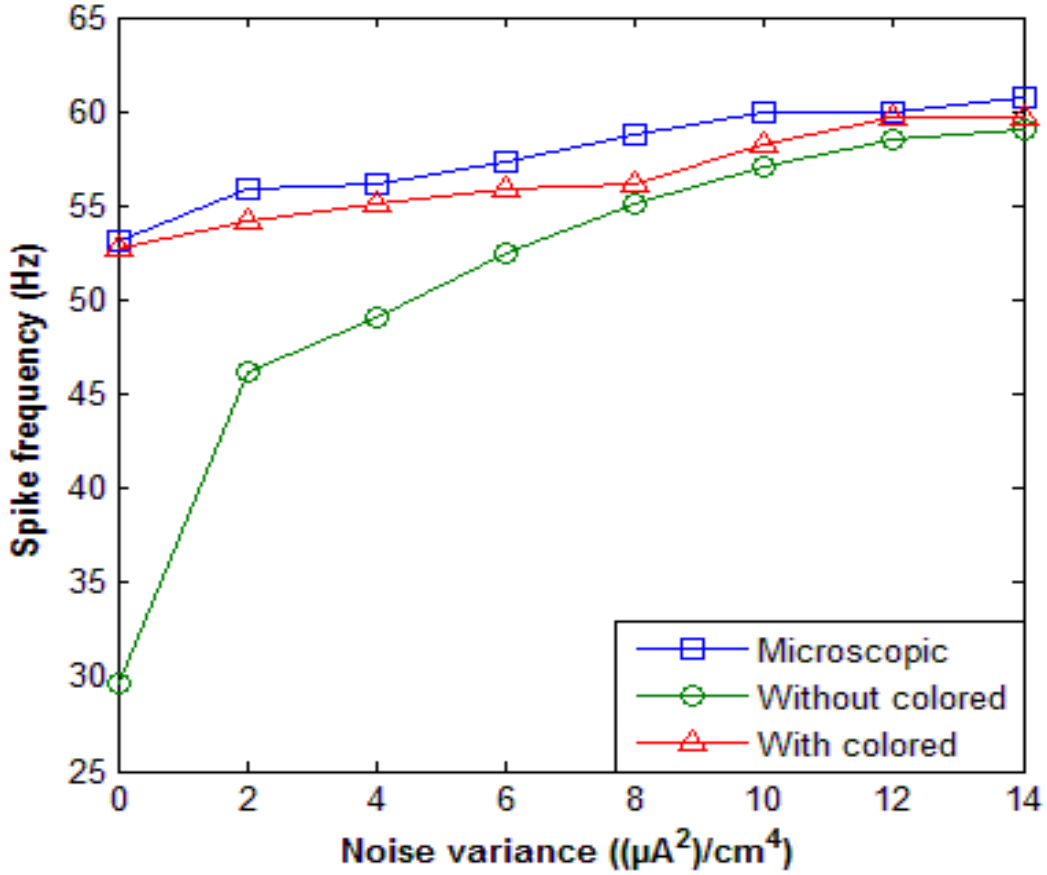


Figure 13: The three curves represent the comparison between the microscopic simulation and the Güler model with colored noise and without colored noise terms.The membrane size for potassium is 1,800 and for sodium is 6,000, $I_{base}$ =6, the simulation time window is 5 seconds.

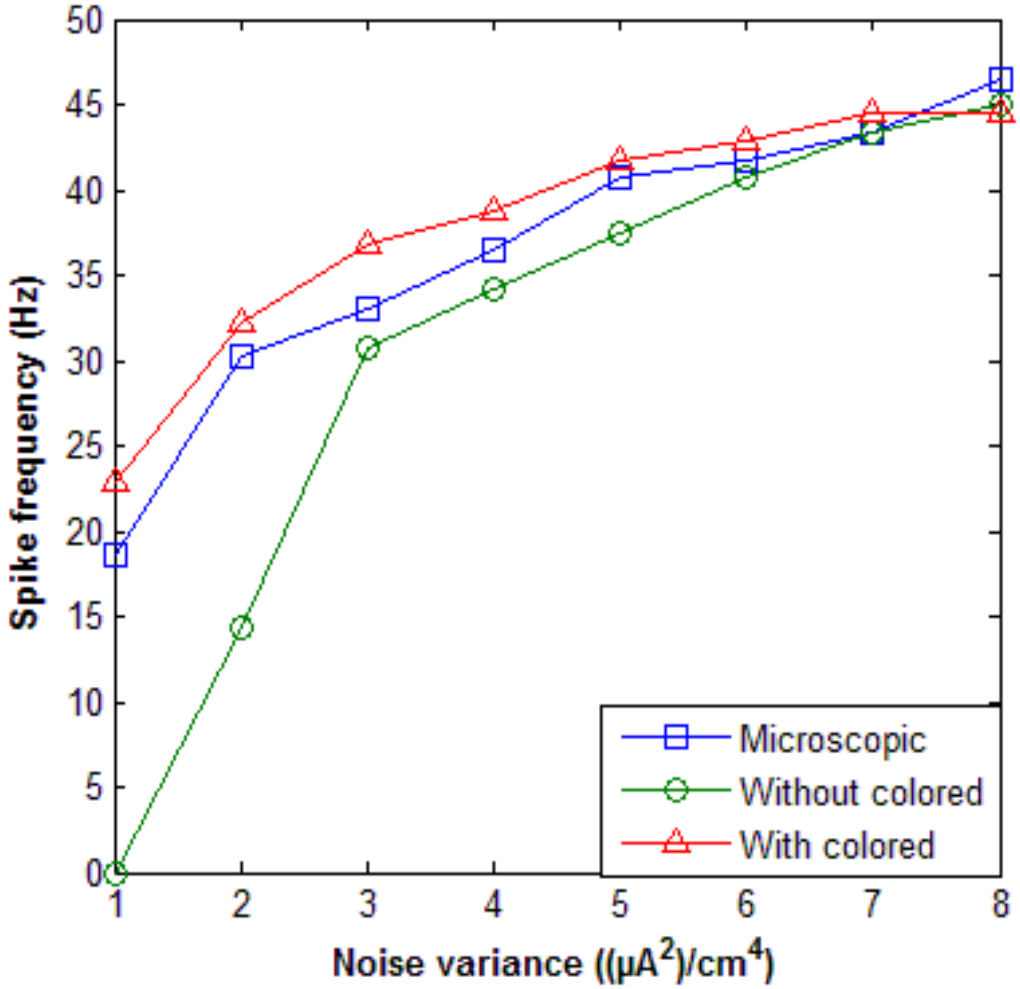


Figure 14: The three curves represent the comparison between the microscopic simulation and the Güler model with colored noise and without colored noise terms. The membrane size for potassium is 2700 and for sodium is 9000, $I_{base}$ =2, the simulation time window is 5 seconds.

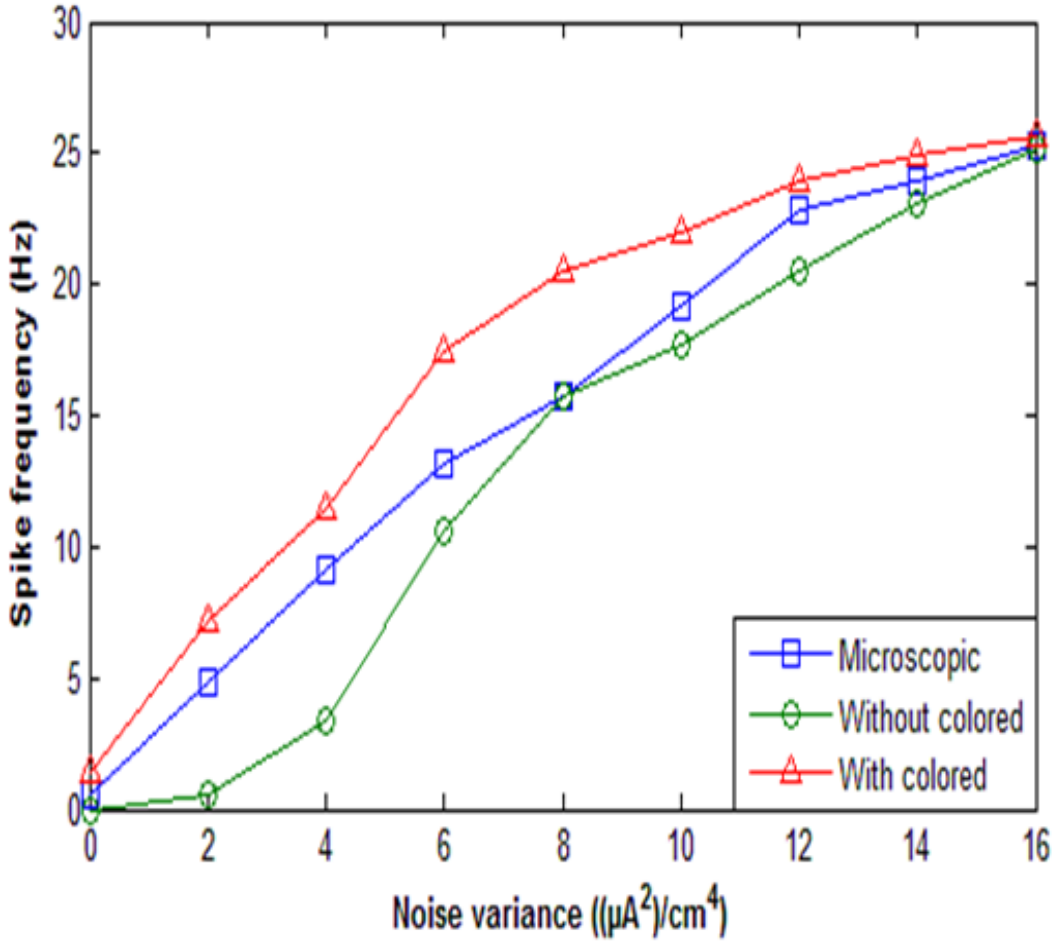


Figure 15: Showing in this figure the membrane size for potassium is 1800 and for sodium is 6000, $I_{base}$ =-2. In addition, the three curves represent the comparison between the microscopic simulation and the Güler model with colored noise and without colored noise terms, in 5 seconds time window.

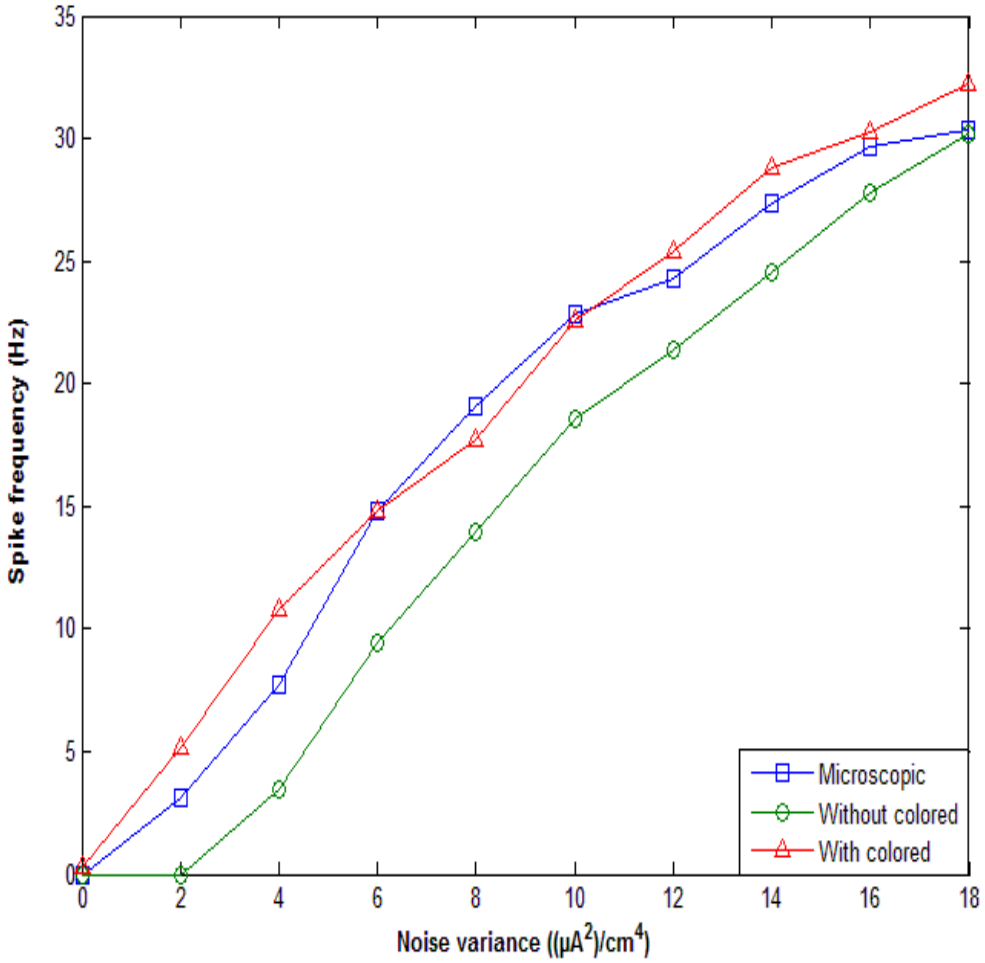


Figure 16: The three curves represent the comparison between the microscopic simulation and the Güler model with colored noise and without colored noise terms. The membrane size for potassium is 2,700 and for sodium is 9,000 $I_{base}$ =-2, the simulation time window is 5 seconds.

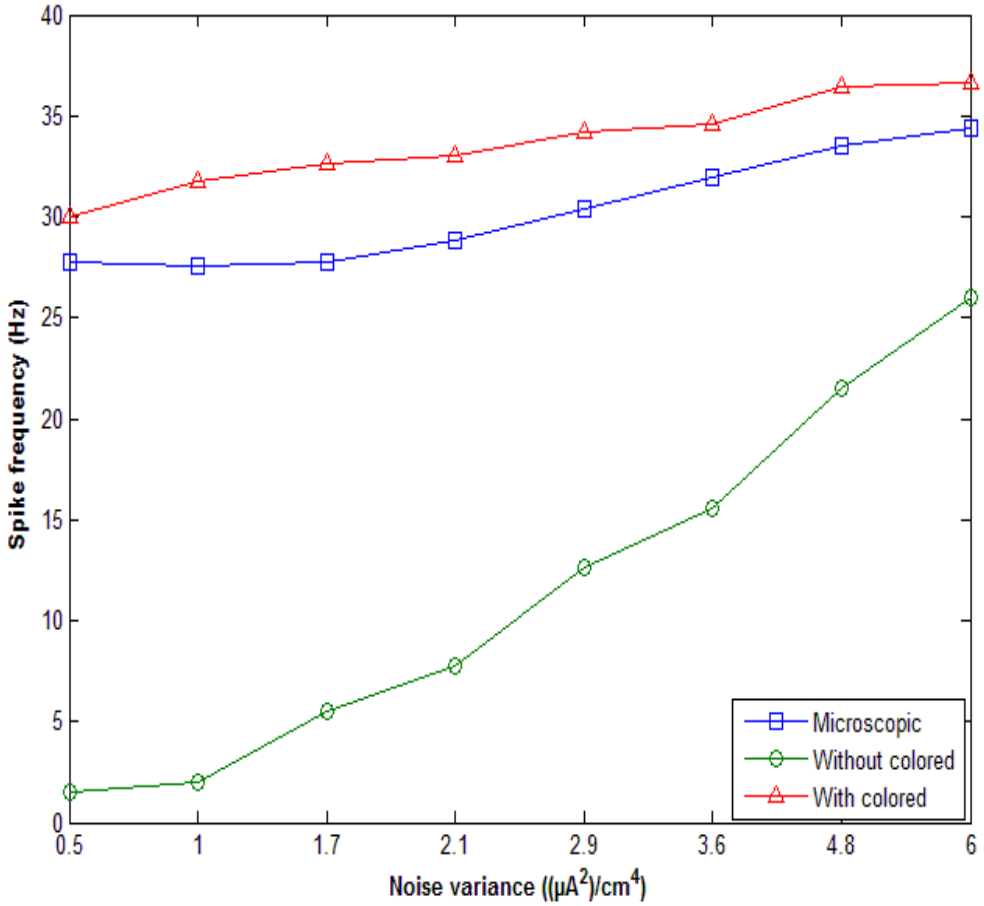


Figure 17: Mean spiking rates against the noise variance. The three curves represent the comparison between the microscopic simulation and the Güler model with colored noise and without colored noise terms. The membrane size for potassium is 600, for sodium is 2000 and $I_{base}$ = 0, in 5 seconds time window. In this figure different noise variance used to show the comparison between the three curves.

Calculating the relative difference between two numbers with $I_{base}$=20, and $I_{base}$=100. When comparing two numbers, subtracting the smaller from the larger yields the difference between them. Examples:

| | |
|---|---|
| 5 | 101 |
| -3 | -99 |
| 2 | 2 |

In both cases above, the difference is the same, (2) and for some purposes, that difference of 2 tells us all we need to know. But there is at least one sense in which the numbers 99 and 101 are closer to each other than are the numbers 3 and 5.

- The relative difference between 5 and 3 is (5-3)/4 =2/4 =.5
- The relative difference between 101 and 99 is (101-99)/100 = 2/100 = .02

Calculating relative differences for spike frequency (Hz), with $I_{base}$ =20, and for spike frequency (Hz), with $I_{base}$ =100, as shown in Table 3.

We can see that the relative differences between each spike frequency numbers will be small, which is mean that even the numbers of spike frequency was big, we can use relative differences between them. So after we use this process, we will get small distance between microscopic simulations, with colored and without colored.

Table 3: Relative differences between spike frequency1, and spike frequency2.

| Spike frequency 1 | $I_{base}$ | Spike frequency 2 | $I_{base}$ |
|---|---|---|---|
| $\frac{(82-81)}{81.5} = 0.0122$ | 20 | $\frac{(20-10)}{15} = 0.6666$ | 100 |
| $\frac{(83-82)}{82.5} = 0.0121$ | 20 | $\frac{(30-20)}{25} = 0.4$ | 100 |
| $\frac{(84-83)}{83.5} = 0.0119$ | 20 | $\frac{(40-30)}{35} = 0.285$ | 100 |
| $\frac{(85-84)}{84.5} = 0.0118$ | 20 | $\frac{(50-40)}{45} = 0.222$ | 100 |
| $\frac{(86-85)}{85.5} = 0.0116$ | 20 | $\frac{(60-50)}{55} = 0.181$ | 100 |
| $\frac{(87-86)}{86.5} = 0.0115$ | 20 | $\frac{(70-60)}{65} = 0.153$ | 100 |
| $\frac{(88-87)}{87.5} = 0.0114$ | 20 | $\frac{(80-70)}{75} = 0.133$ | 100 |

With the results we calculate mean spiking rates opposing the noise variance, now we will calculate the coefficient of variation up against the noise variance.

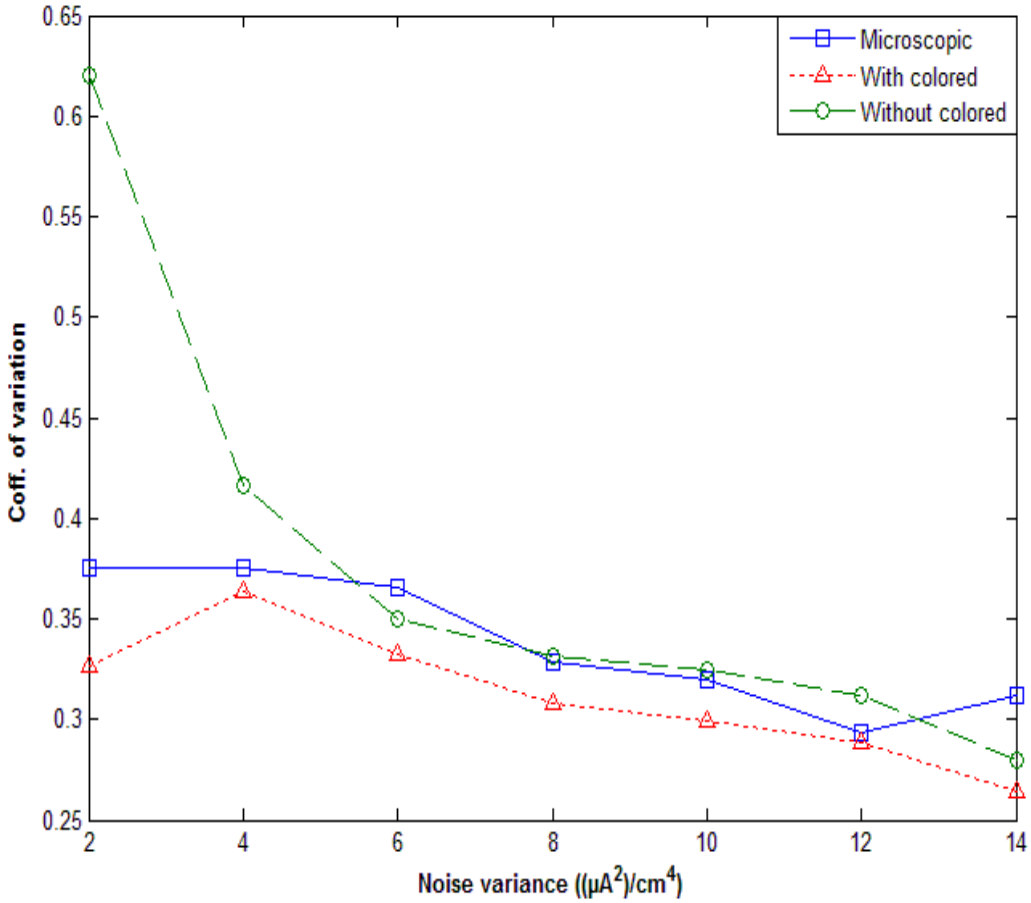


Figure 18: The coefficient of variation against the noise variance, displayed by a membrane patch comprised of 900 potassium channels and 3, 000 sodium channels. The completely stochastic actual dynamics was used. The three plots shown correspond to: with colored and without colored and microscopic simulations. The averages were computed over a 5 sec. time window.

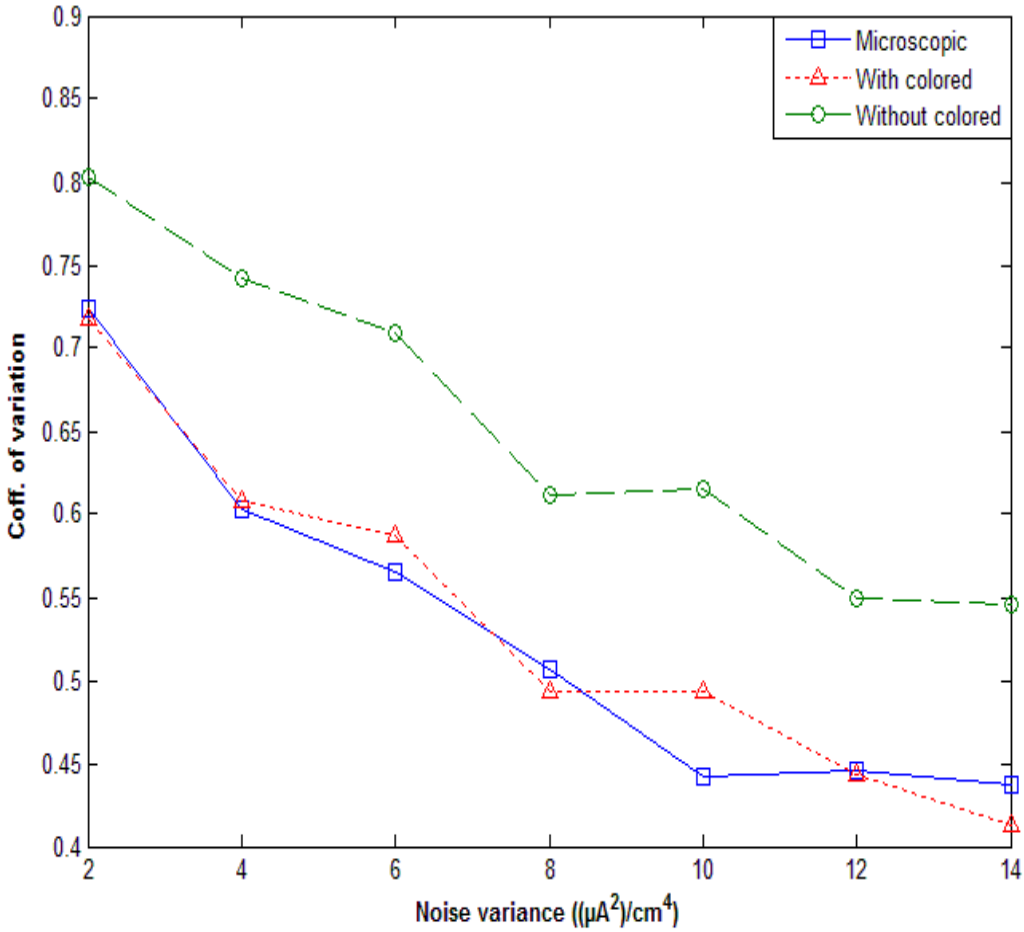


Figure 19: The coefficient of variation against the noise variance, displayed by a membrane patch comprised of 1,800 potassium channels and 6,000 sodium channels. The completely stochastic actual dynamics was used. The three plots shown correspond to: with colored and without colored and microscopic simulations. The averages were computed over a 5 sec. time window.

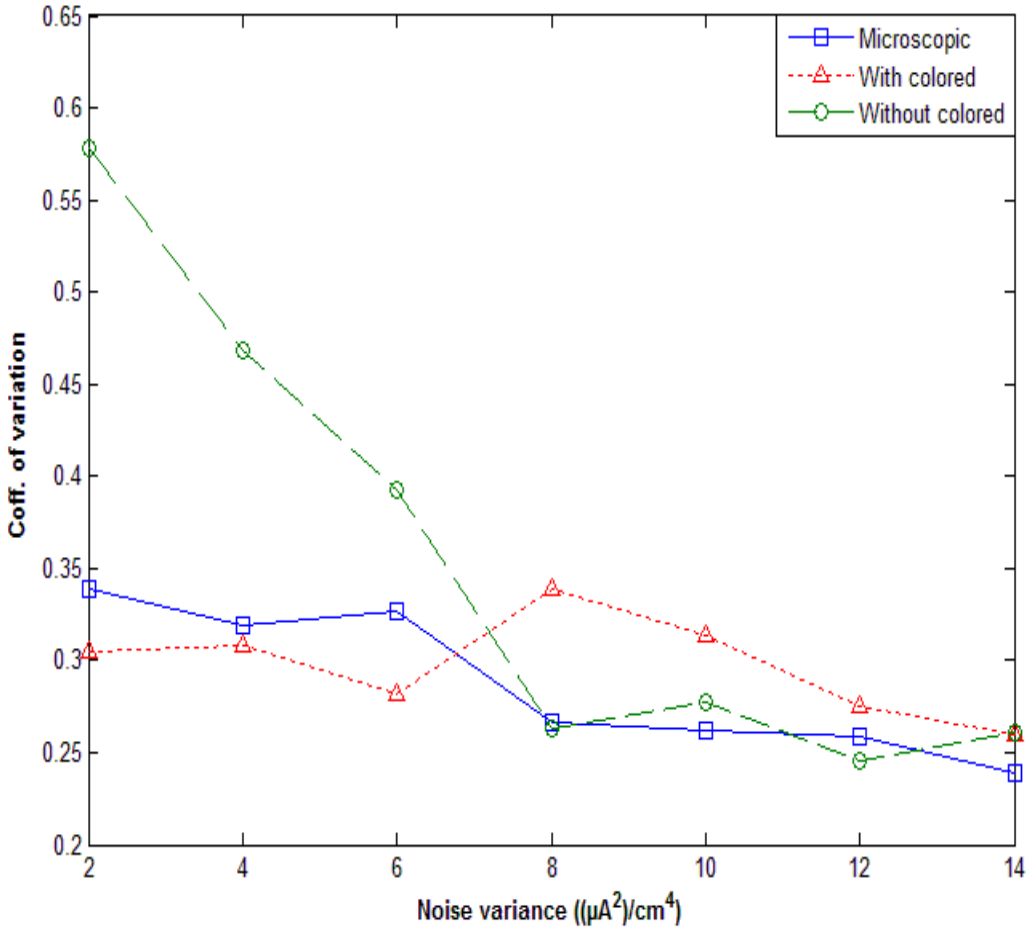


Figure 20: The coefficient of variation against the noise variance, displayed by a membrane patch comprised of 2,700 potassium channels and 9,000 sodium channels. The completely stochastic actual dynamics was used. The three plots shown correspond to: with colored and without colored and microscopic simulations. The averages were computed over a 5 sec. time window.

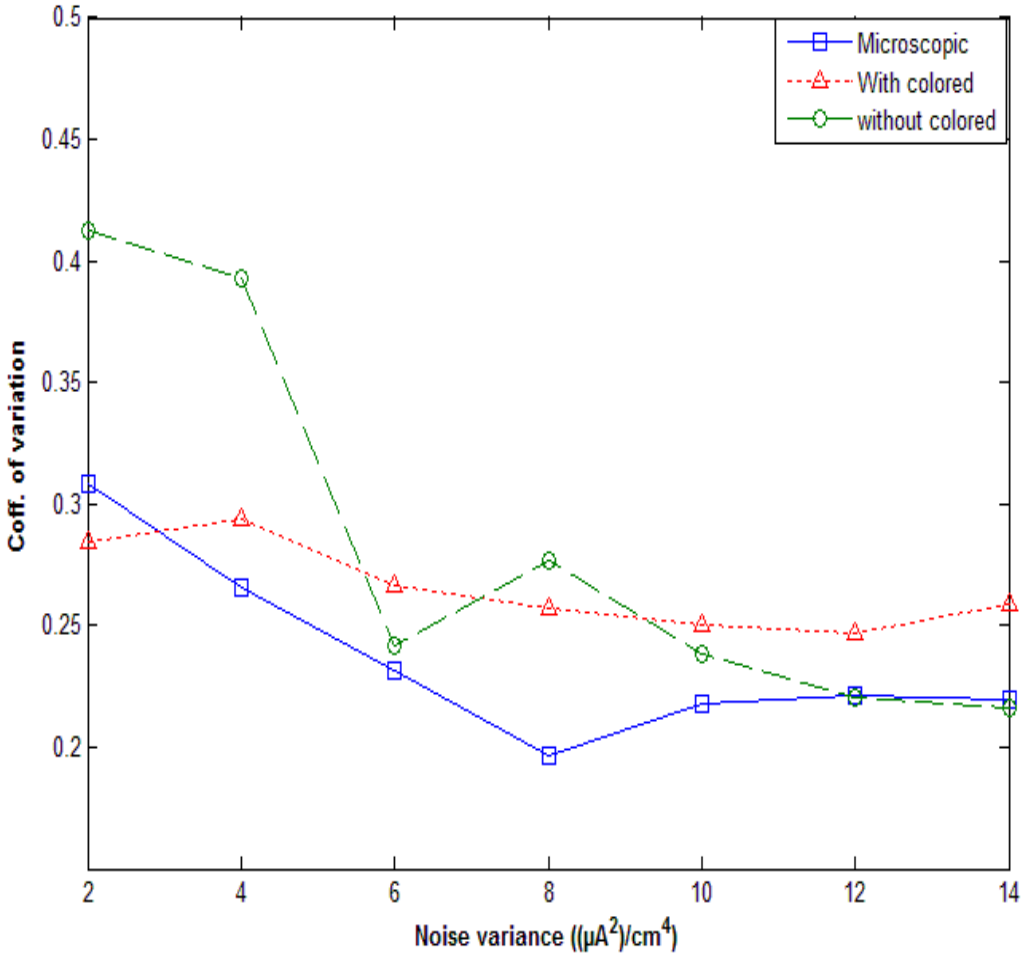


Figure 21: The coefficient of variation against the noise variance, displayed by a membrane patch comprised of 3,210 potassium channels and 1,0700 sodium channels. The completely stochastic actual dynamics was used. The three plots shown correspond to: with colored and without colored and microscopic simulations. The averages were computed over a 5 sec. time window.

## 6.2 Future works

As for the concern of further work in future, there is a huge demand to use clossal membrane inside the subsequent with size of more than 4,000 potassium channels along with increased noise variance, also the disparate $I_{base}$ as the stochastic HH equation that must be contrasted along with the colored noise term and the microscopic as well. However, for coefficient of variation, it is better to utilize small membrane size.

# Chapter 7

# CONCLUSION

So far as in this study, we have concluded that the colored noise neuron model was studied well under the influence of varying input signal. In the beginning, it was observed that with single ion channels, multiplicity of the gates plays an important role that in return motivates the NCCP (non-trivially cross correlation persistent). Later it has been found that to be the main cause in the unusual increases in the cell excitability and in spontaneous firing membrane size should be small enough (Güler, 2011). Moreover, it was discovered that NCCP keeps on promoting the spontaneous firing even if membrane size is larger, wherever the gate of noise is insufficient for activating the cell. Likewise, this study has also revealed that enhancement of the spike coherence was due to the presence of the NCCP.

According to the experimental results, the spiking rate generated from the model is very close to the one from the actual simulation, doesn't matter whatever the membrane size was, and unlike the stochastic HH model it was completely distinct from the actual neuron spikes. In contrast, the rate generated through an increase in noise variance, the stochastic HH equation without the colored term but with spikes was almost similar as compared to the spikes from the model.

Experiment results also highlight the mean spiking rates against noise, that was displayed by a different membrane size, with different $I_{base}$, and with different noise

variance, in which three curves represent the competition between the microscopic simulation with the stochastic HH equation and the colored term, and also the colored term model has worked quite similar to the microscopic simulations with $I_{base}$ (0, 2, 4, 6) but with $I_{base}$ (-2), the colored term has performed like the microscopic simulations and even the HH equation was not too much different from the actual neuron spikes when there was increased in noise variance. With $I_{base}$= 20 or 100, the colored noise has worked differently to the microscopic simulations, because $I_{base}$ was large and noise variance was small.

We will squeeze our findings by concluding that the presented coefficient of variation computations in our studies was conducted for an exemplar membrane patch. It's been driven out that the spike coherence in colored term at the same level was as the coherence in the microscopic simulation scheme. Even though the spiking from stochastic HH equations is less coherent as significantly larger coefficient of variation values, but when there is increase in noise variance the stochastic HH equations will be the smaller coefficient of variation values. Therefore it can be said that, an increasing noise variance is a decrease in the coefficient of variation.

.

# REFERENCE


Abbot, D. P. (2002). theorretical Neuroscience Computation and mathematical modeling of neural system. *MIT* press.

Bezrukov, S. (1995). Noise-induced enhancement of signal transduction across voltage-dependent ion channels. *Nature, 378, 362–364.*

Chow, C. C. (1996). Spontaneous action potentials due to channel fluctuations. *Biophysical Journal, 71,3013–3021.*

DeFelice, L. J. (1992). Chaotic states in a random world: Relationship between the nonlinear differential equations of excitability and the stochastic properties of ion channels. *Journal of Statistical Physics, 70, 339–354.*

Diba, K. L. (2004). Intrinsic noise in cultured hippocampal neurons: Experiment and modeling. *Journal of Neuroscience, 24, 9723–9733.*

Dorval, A. D. (2005). Channel noise is essential for perithreshold oscillations in entorhinal stellate neurons. *Journal of Neuroscience, 25, 10025–10028.*

Faisal, A. A. (2007). Stochastic simulations on the reliability of action potential propagation in thin axons. *PLoS Computational Biology, 3, 79.*

Faisal, A. S. (2008). Noise in the nervous system. *nervous system. Nature Reviews Neuroscience, 9, 292–303.*

Güler, M. (2007). Dissipative stochastic mechanics for capturing neuronal dynamics under the influence of ion channel noise: Formalism using a special membrane. *Physical Review E, 76,041918(17).*

Güler, M. (2008). Detailed numerical investigation of the dissipative stochastic mechanics based neuron model. *Journal of Computational Neuroscience, 25, 211–227.*

Güler, M. (2011). Persistent membranous cross correlations due to the multiplicity of gates in ion channels. *Journal of Computational Neuroscience, 31,713-724.*

Güler, M. (2013). Stochastic Hodgkin-huxley equations with colored noise terms in the conductances. *Neural Computation, 25, 46-74.*

Hille, B. (2001). Ionic channels of excitable membranes (3rd ed.). *Massachusetts: Sinauer Associates.*

Hodgkin, A. L. (1952). A quantitative description of membrane current and its application to conduction and excitationin in nerve. Journal of Physiology. *(London.Print), 117, 500–544.*

Izhikevich, E. M. (2007). Dynamical Systems in Neuroscience:The Geometry of Excitability and Bursting. *San Diego, California.*

Jacobson, G. A. (2005). Subthreshold voltage noise of rat neocortical pyramidal neurones. *Journal of Physiology, 564,145–160.*

Johansson, S. (1994). Single-channel currents trigger action potentials in small cultured hippocampal neurons. *Proceedings of National Academy of Sciences USA, 91, 1761–1765.*

Jung, P. (2001). Optimal sizes of ion channel clusters. *Europhysics Letters, 56, 29–35.*

Koch, C. (1999). Biophysics of computation: Information processing in single neurons. *Oxford: Oxford University Press.*

Kole, M. H. (2006). Single Ih channels in pyramidal neuron dendrites: Properties, distribution, and impact on action potential output. *Journal of Neuroscience, 26, 1677–1687.*

Lynch, J. (1989). Action potentials initiated by single channels opening in a small neuron (rat olfactory receptor). *Biophysical Journal, 55, 755–768.*

Ochab-Marcinek, A. S. (2009). Noise-assisted spike propagation in myelinated neurons. *Physical Review E, 79, 011904(7).*

Özer, M. (2006). Frequency-dependent information coding in neurons with stochastic ion channels for subthreshold periodic forcing. *Physics Letters A, 354, 258–263.*

Rowat, P. F. (2004). State-dependent effects of Na channel noise on neuronal burst generation. *Journal of Computational Neuroscience, 16, 87–112.*

Rubinstein, J. (1995). Threshold fluctuations in an N sodium channel model of the node of Ranvier. *Biophysical Journal,68, 779–785.*

Sakmann, B. (1995). Single-channel recording (2nded.). *New York: Plenum.*

Schmid, G. G. (2001). Stochastic resonance as a collective property of ion channel assemblies. *Europhysics Letters, 56, 22–28.*

Schneidman, E. F. (1998). Ion channel stochasticity may be critical in determining the reliability and precision of spike timing. *Neural Computation, 10, 1679–1703.*

segev I., J. B. (2003). Cable and compartment models of dendritic trees in bower. *the book of genesis 5:55.*

Sigworth, F. J. (1980). The variance of sodium current fluctuations at the node of Ranvier. Journal of Physiology. *(London Print), 307, 97–129.*

Strassberg, A. F. (1993). Limitations of the Hodgkin–Huxley formalism: Effects of single channel kinetics on transmembrane voltage dynamics. *Neural Computation 5, 843–855.*

Whishaw, K. B. (2012). Fundamentals of Human Physiology FOURTH EDITION. *Virginia United States.*

White, J. A. (1998). Noise from voltage-gated ion channels may influence neuronal dynamics in the entorhinal cortex. *Journal of Neurohysiology, 80, 262–269.*

Zeng, S. (2004). *Mechanism for neuronal spike generation by small and large ion channel clusters. Physical Review E, 70, 011903(8).*

Sengupta, B. Laughlin SB, Niven JE. *Phys Rev E. 2010;81:011918.*

Rowat, P. *Neural Comput. 2007;19:1215.*

Brunel, N. Chance FS, Fourcaud N, Abbott LF. *Phys Rev Lett. 2001;86:2186.*

Schmid, G. P. H. (2007). Intrinsic coherence resonance in excitable membrane patches. In Mathematical Biosciences (pp. 236-244*). Augsburg: Institut fu¨ r Physik, Universita¨ t Augsburg, Theoretische Physik I,.*

Guggisberg, A. G. S. S. Dalal, A. M. Findlay, and S. S. Nagarajan, "Highfrequency oscillations in distributed neural networks reveal the dynamics of human decisiomaking*," Frontiers in Human Neuronscience, March 2008*.

Villarreal, M. R. "Diagram of a typical myelinated vertebrate neuron." *July 2007.*

Leonardo, G. "Schematic view of an idealized action potential," *August 2006.*

Bailey, J. "Towards the neurocomputer: an investigation of VHDL neuro models," Ph.D. dissertation, University of Southampton, *February 2010.*

Stuart and B. Sakmann, G. J. "Active propagation of somatic action potentials into pyramidal cell dendrites." *Nature, vol. 367, no. 6458, pp. 69–72, January 1994.*

# APPENDIX

```
#include <stdio.h>

#include <stdlib.h>

#include <math.h>

#include <ctype.h>

#define Two_PI 6.2832

#define Max_No_Paths 10000

//'D' means potassium dynamics is Deterministic

const char potassium_dyn = 'S';

//'D' means sodium dynamics is Deterministic

const char sodium_dyn = 'S';

const char update_s_mode = '+';

//'+' means use Update_b

const char update_b_mode = '-';

//'+' means shuffle

char shuffle_mode_n = '-';

char shuffle_mode_mh = '-';

//'+' means convert
```

```
char convert_mode_n = '-';

char convert_mode_mh = '-';

//'+' means renormalizied solution is computed

const char renorm_sol_mode = '+';

//'+' means solve Deterministic HH equations

const char HH_mode = '-';

//'+' means apply Fox-Lu in Deterministic equations

const char Fox_Lu_mode = '-';

//'+' means apply Linaro_et_al in Deterministic equations

const char Linaro_mode = '-';

float Dt_sb = 0.01;

const float Dt_d = 0.005;

const float Cap = 1.;

const float g_K = 36.;

const float E_K = -12.;

const float g_Na = 120.;

const float E_Na = 115.;

const float g_L = 0.3;

const float E_L = 10.6;
```

```
const float Gamma_K = 10;

const float Omega2_K = 150;

const float T_K = 400;

const float Gamma_Na = 10;

const float Omega2_Na = 200;

const float T_Na = 800;

int PrintFreq;

void InitParam(void);

double alpha_n(double V);

double beta_n(double V);

double alpha_m(double V);

double beta_m(double V);

double alpha_h(double V);

double beta_h(double V);

double rhs_V_d_Dot(double V, double n, double m, double h);

double rhs_nDot(double V, double n);

double rhs_mDot(double V, double m);

double rhs_hDot(double V, double m);
```

```
double rhs_V_sb_Dot(double V_z, double n_C, double mh_C);

void Update_s(char f_v);

void Update_b(char f_v);

void Rung_Kutt_Determ(void);

void Rung_Kutt_Fox_Lu(void);

void Rung_Kutt_Linaro(void);

void Rung_Kutt_Renorm(void);

double Random();

float GWN_BM(float Variance);

float GWN_RW(float Variance);

float I_0, I_1;

static int No_P_ch, No_S_ch;

static int No_paths;

static int N_s_4[Max_No_Paths], N_s_3[Max_No_Paths],
    N_s_2[Max_No_Paths], N_s_1[Max_No_Paths], N_s_0[Max_No_Paths];

static int MH_s_31[Max_No_Paths], MH_s_30[Max_No_Paths],
        MH_s_21[Max_No_Paths], MH_s_20[Max_No_Paths],
        MH_s_11[Max_No_Paths], MH_s_10[Max_No_Paths],
        MH_s_01[Max_No_Paths], MH_s_00[Max_No_Paths];
```

```
static int N_s_g[Max_No_Paths], M_s_g[Max_No_Paths],
        H_s_g[Max_No_Paths];
static double N_b_4[Max_No_Paths], MH_b_31[Max_No_Paths];
static int N_b_g[Max_No_Paths], M_b_g[Max_No_Paths],
        H_b_g[Max_No_Paths];
static double n_Ds[Max_No_Paths];
static double m_Ds[Max_No_Paths], h_Ds[Max_No_Paths];
static double n_Db[Max_No_Paths];
static double m_Db[Max_No_Paths], h_Db[Max_No_Paths];
static double V_s[Max_No_Paths];
static double V_b[Max_No_Paths];
static double V_d, n_d, m_d, h_d;
static double V_r, n_r, m_r, h_r;
static double q_K = 0.0, p_K = 0.0, q_Na = 0.0, p_Na = 0.0;
static double z_K[5]={0.0}, z_Na[8]={0.0};
unsigned int Max_Time;
int Four_No_P_ch, Three_No_S_ch;
double Sqrt_Dt_d;
```

```
/*----------------------------------------*/

float Input_Curr(double Time)

{

 unsigned long count;

 float input_var = 9;



/*----------------------------------------*/

double rhs_V_r_Dot(double V_r, double n_r, double m_r, double h_r)

{

 double value, n_rP4, m_rP3;

 n_rP4 = pow(n_r, 4);

 m_rP3 = pow(m_r, 3);

 aux_Psi_K_Ren = n_rP4;

 aux_Psi_Na_Ren = m_rP3*h_r;

 if(potassium_dyn != 'D')

 {

  if(n_rP4 < 1.0)

   aux_Psi_K_Ren+=0;// sqrt(n_rP4*(1-n_rP4)/No_P_ch)*q_K;

 }
```

```
 if(sodium_dyn != 'D')

 {

  if(m_rP3 > 0.0 && m_rP3 < 1.0)

   aux_Psi_Na_Ren+=0;//sqrt(m_rP3 *(1-m_rP3)/No_S_ch)*h_r*q_Na;

 }

 value = -g_K*aux_Psi_K_Ren*(V_r - E_K) -

         g_Na*aux_Psi_Na_Ren*(V_r - E_Na) - g_L*(V_r - E_L) + I_1;

 value /= Cap;

 return value;

}

double diffus_n, diffus_m;

/*----------------------------------------*/

#include <stdio.h>

#include <stdlib.h>

#include <math.h>

#include <ctype.h>

float range_begin=500;

float range_end=10000000;

float threshold = 50.;
```

```
long int density_s=0, density_b=0, density_d=0, density_r=0;

float V_s, V_b, V_d, V_r;

char state_s='b', state_b='b', state_d='b', state_r='b';

main()

{

 unsigned int i = 0;

 FILE *infile;

 char infilename[100];

 char dumstr[601];

 float Time;

 printf("ENTER THE DATA FILE NAME => ");

 fgets(infilename,99,stdin);

 i=0; while(infilename[i] != '\n') i++;

 infilename[i] = '\0';

 infile = fopen(infilename, "r");

 do

 {

  fgets(dumstr, 600, infile);

  if(dumstr[2] == 'I' && dumstr[4] == '=')
```

```
 fprintf(stdout, "\n   I =%c%c%c%c%c%c\n",
  dumstr[5], dumstr[6], dumstr[7], dumstr[8],
  dumstr[9], dumstr[10]);
}while(dumstr[0] == '#');
fprintf(stdout, "\n   Please wait ...\n");
while(fscanf(infile,"%f", &Time) != EOF)
{
 if(Time > range_end) break;
 if(Time < range_begin)
 {
  fgets(dumstr, 600, infile);
  continue;
 }
 fscanf(infile,"%f %f %f %f", &V_s, &V_b, &V_d, &V_r);
 fgets(dumstr, 600, infile);
 if(V_s > threshold + 10.)
 {
  if(state_s == 'b') density_s++;
  state_s = 'a';
```

```
}
 else if(V_s < threshold - 10.) state_s = 'b';
 if(V_b > threshold + 10.)
 {
  if(state_b == 'b') density_b++;
  state_b = 'a';
 }
 else if(V_b < threshold - 10.) state_b = 'b';
 if(V_d > threshold + 10.)
 {
  if(state_d == 'b') density_d++;
  state_d = 'a';
 }
 else if(V_d < threshold - 10.) state_d = 'b';
 if(V_r > threshold + 10.)
 {
  if(state_r == 'b') density_r++;
  state_r = 'a';
 }
```

```
  else if(V_r < threshold - 10.) state_r = 'b';

 }

 fprintf(stdout, "\nSpike frequencies over the time interval"

    " [%3.1f - %4.1f] are:\n\n", range_begin, Time);

/*

fprintf(stdout, "V_s: %ld\n", density_s);

fprintf(stdout, "V_b: %ld\n", density_b);

fprintf(stdout, "V_d: %ld\n", density_d);

fprintf(stdout, "V_r: %ld\n", density_r);

*/

 fprintf(stdout, "V_s: %6.2f\n",

 1000.*density_s/(Time-range_begin));

 fprintf(stdout, "V_b: %6.2f\n",

      1000.*density_b/(Time-range_begin));

 fprintf(stdout, "V_r: %6.2f\n",

      1000.*density_r/(Time-range_begin));

 fprintf(stdout, "V_d: %6.2f\n",

      1000.*density_d/(Time-range_begin));

}
```